University of Alberta

The Geometry and Diffraction of the Pinwheel Tiling

by

Derek Lawrence Lindsay Postnikoff 

A thesis submitted to the Faculty of Graduate Studies and Research in partial fulfillment of the requirements for the degree of Master of Science.

in

Mathematics

Department of Mathematical and Statistical Sciences

Edmonton, Alberta

Fall 2004

Your file Votre référence
ISBN: 0-612-95832-9
Our file Notre référence
ISBN: 0-612-95832-9

Acknowledgements

This document would not exist in any form without the expert supervision of Dr. Robert V. Moody. His legendary insight and patient tutelage have been a prodigious source of knowledge and inspiration. He has earned my undying gratitude and respect several times over.

Special thanks also go to my colleagues Nicolae Strungaru and Jeong-Yup Lee. Many of their wise comments and suggestions permeate this work, and I am greatly indebted to them for these generous contributions. Additionally, I would like to take this opportunity to express my appreciation to Dr. Michael Baake and Dr. Rajiv Mandal for their interest and sagacious observations.

I owe a debt of gratitude to the support staff of the Department of Mathematical and Statistical Sciences, particularly Dona Guelzow, for their considerable assistance with all things administrative.

Finally, I could not have survived this process without the loving support of my family and friends. Their myriad contributions – from assisting with proofreading to engaging in prolonged discussions to providing tasty comestibles – have been enthusiastic and invaluable. In particular, I would like to thank my wife Thora Gudmundson for her unwaivering love and devotion.

The majority of the research for this thesis was funded by the generous support of the Alberta Ingenuity Fund.

This thesis was typeset using LaTeX.

Table of Contents

List of Figures

Chapter 1 - Introduction

Mathematics is the science of patterns. A class of two dimensional visual patterns known as tilings has been an important element of human existence throughout history. In recent years, the mathematical study of tilings has been promoted from a whimsical curiosity to a serious inquiry. This transformation can be largely attributed to the successful adoption of tiling models in crystallography and materials science, and the discovery of well ordered aperiodic structures in mathematics and in nature. One of the most intriguing aperiodic tilings is the Conway-Radin pinwheel tiling, a structure exhibiting infinitely many orientations amongst its $1:2:\sqrt{5}$ right triangular tiles.

This thesis is a mathematical examination of the pinwheel tiling. We begin by providing a brief introduction to tilings in general to provide some context for the ensuing discussion. For aeons, human beings have been covering their walls and floors with ceramic and stone tiles to protect and decorate them. The ultimate decorative tiling is a mosaic, a picture created from hundreds of stone chips of many sizes, shapes, and colours. On the other hand, a perfectly functional floor tiling might be composed of large uniform square flagstones arranged in a repetitive pattern. Tilings of varying levels of complexity play an important role in art and architecture. We find a similar range of tilings in nature: the simple periodicity found in a honeycomb or fish scales contrasts with the disorder present in sea foam or cracked mudflats. These examples demonstrate the variety and ubiquitousness of tilings.

The mathematical definition of tiling is formulated to correspond to the physical patterns bearing the same name. A tiling is a collection of compact subsets of $\mathbb{R}^2$ that is both a packing and a covering; that is, the interiors of any two tiles do not intersect, and the union of all tiles is the plane. All mathematical tilings are assembled according to some kinds of rules. Some of the most significant techniques used to create mathematical tilings are the substitution method, the cut-and-project method, and the matching rule method. Historically, most mathematical tilings and physical models involving tilings were constructed according to matching rules. Basically put, this method fits together tiles from finitely many different congruency classes (called prototiles) according to a set of matching rules to construct a tiling. Clearly, matching rule tilings tend to be well ordered. Until recently, the majority of well ordered tilings known were periodic.

The advent of group theory revolutionized the mathematics of tilings. Focus shifted from the shapes and configurations of tiles to the rich symmetries present in the periodic patterns. This movement culminated in the classification of the 17

planar symmetry groups – as well as the 230 three dimensional space groups – in the late nineteenth century [6]. An important part of this classification theorem is the Crystallographic Restriction which states that the only rotational symmetries compatible with periodicity have order $2, 3, 4$, or 6. Since the long range order of any periodic tiling is completely determined by its symmetry group, the study of periodic tilings was reduced to the study of local configurations. While a few dedicated souls toiled on creating new tilings and proving results concerning local configurations, it would take the discovery of a new kind of long range order to revive the study of tilings to more than a hobby.

In the early twentieth century, Harald Bohr developed the theory of almost periodic functions, thereby introducing the concept of aperiodic order [15]. However, it was 1961 when Hao Wang finally posed the question "Is it possible to have a finite set of prototiles that only tile aperiodically?" [13]. Wang's motivation came from decidability problems in mathematical logic, and he conjectured that the answer to his question was "no." However, Wang's student Robert Berger proved the existence of a set of 20,426 prototiles that cannot tile periodically [8]. While several other aperiodic examples with significantly fewer prototiles were discovered shortly thereafter, the most celebrated aperiodic tiling was conceived in 1974: the Penrose kite and dart tiling. This tiling consists of only two prototiles that must tile aperiodically [8]. It remains an open question whether an aperiodic tiling of the plane by a single prototile exists.

In 1984, the first physical substance demonstrating long-range aperiodic order was discovered by Shechtman et al. [17]. The material in question, an alloy of aluminum and manganese, was bestowed with the epithet "quasicrystal" due to its crystal-like (that is, pure point) diffraction pattern that simultaneously revealed icosahedral symmetries proven to be incompatible with a periodic lattice structure. This material displayed some physical characteristics like those of periodic crystals and others similar to those of amorphous glasses. By chance, the diffraction pattern of this quasicrystal resembled the diffraction of the Penrose tiling. This fortuitous coincidence brought new life to the mathematical study of tilings.

The past two decades have witnessed the development of a remarkable collection of mathematical tools designed to help explain this new form of order: a new theory of diffraction based on measures, the application of dynamical systems, a wealth of new ideas concerning substitution systems, the introduction of non-commutative geometry into crystallography, and so on. However, despite a lack of overall translational symmetry, almost all of this theory depends on the premise that the underlying

symmetries are fundamentally translational in nature. In particular, this implies that the orientational order observed must be finite. It is somewhat astonishing that in physical quasicrystals and objects like Penrose tilings alike, there are only finitely many orientations of local clusters of atoms or tiles.

Ten years after the discovery of quasicrystals, the tiling research explosion resulted in the discovery of a new aperiodic tiling. Unlike some previous aperiodic tilings that demonstrated forbidden rotations of finite order in their orientational symmetry, the Conway-Radin pinwheel tiling was constructed specifically to possess infinitely many tile orientations [13]. In his original paper, Charles Radin formulated the matching rules for the pinwheel tiling. Assuming that we are permitted to reorient prototiles, approximately 100,000 are required to construct the pinwheel (as estimated by Penrose in [10]; no exact computation could be found in the literature). There is a much easier way to arrive at the pinwheel tiling than by using Radin's matching rules, and that is by considering it as a substitution tiling.

1.1 Substitution Tilings

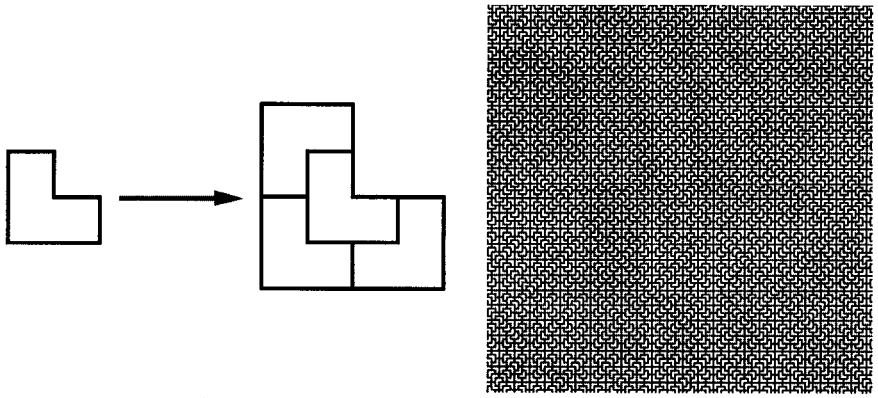

Figure 1: The chair substitution and chair tiling

The substitution method for constructing a tiling is basically an algorithm for decomposing an inflated version of each prototile into tiles. To create a tiling, one starts with one prototile and applies the inflation-decomposition algorithm iteratively. Figure 1(a) illustrates such an algorithm while (b) is a patch of the tiling created using that algorithm; this aperiodic tiling is usually called the chair tiling. In this tiling, there are four types of prototile up to translation: the 'chair' in its four orientations.

There is an extensive canon of literature on substitution systems available that applies to substitution tilings.

We are only interested in fixed point substitutions; this condition ensures that the limit of our successive iterates exists if we start with the correct prototile, and that the resulting tiling of space is invariant under the substitution. Generally, we should start with a prototile that contains a copy of itself in its interior after finitely many iterations.

One cannot mention substitution tilings without referring to Chaim Goodman-Strauss' paper relating substitution tilings and matching rules [7].

1.2 The Pinwheel Tiling as a Substitution

The pinwheel tiling was first conceived as a substitution tiling by John H. Conway. Charles Radin later developed the matching rules that determine the same structure [13]. It is an aperiodic tiling of the plane by $1 : 2 : \sqrt{5}$ right triangles and may be constructed by iterating the following substitution rule:

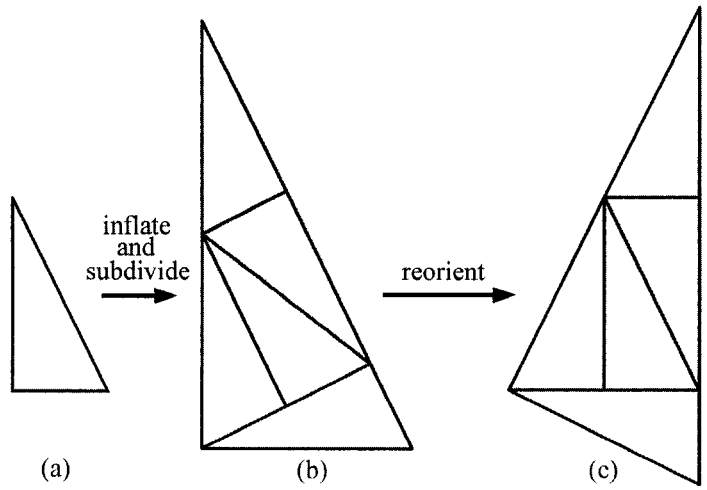

Figure 2: The pinwheel substitution

As you can see, this substitution consists of the standard inflation and subdivision but also requires a second step: a rotation that aligns the new central triangle with the original tile. This extra step is necessary as we require the pinwheel substitution to have a fixed point. The rotation step turns out to be indicative of the unique features of the pinwheel tiling that make it an exceptional object, as will become apparent in the subsequent chapters.

1.3 Outline

In Chapter 2, we provide a mathematical introduction to the pinwheel tiling and lay the foundation for the rest of the thesis. This primarily involves establishing an equivalence between tiles and control points that will facilitate our computations. We also show that the pinwheel tiles occur in infinitely many orientations within the tiling. A new theorem demonstrating that the subsets of the pinwheel tiling defined by chirality are mutually locally derivable is presented. Chapter 3 is dedicated to showing that this sequence of orientations is uniformly distributed, a result that was previously established by Radin. All subsequent calculations rely heavily on this result.

The remainder of the thesis focuses on calculating the diffraction of the pinwheel tiling. Diffraction is a fundamental and widely used technique utilized by scientists and mathematicians to probe the order properties of a structure. The diffraction of a structure, by definition, is the Fourier transform of its autocorrelation. Chapter 4 calculates the autocorrelation measure of the pinwheel tiling, which is interesting in its own right as well as being an intermediary in the process of obtaining the diffraction. Chapter 5 summarizes what we know about the diffraction, and indicates some possible avenues of continued inquiry. While we do not completely solve the mystery of the pinwheel in the following pages, we do make some significant progress in that direction and provide a solid staging point for those who follow.

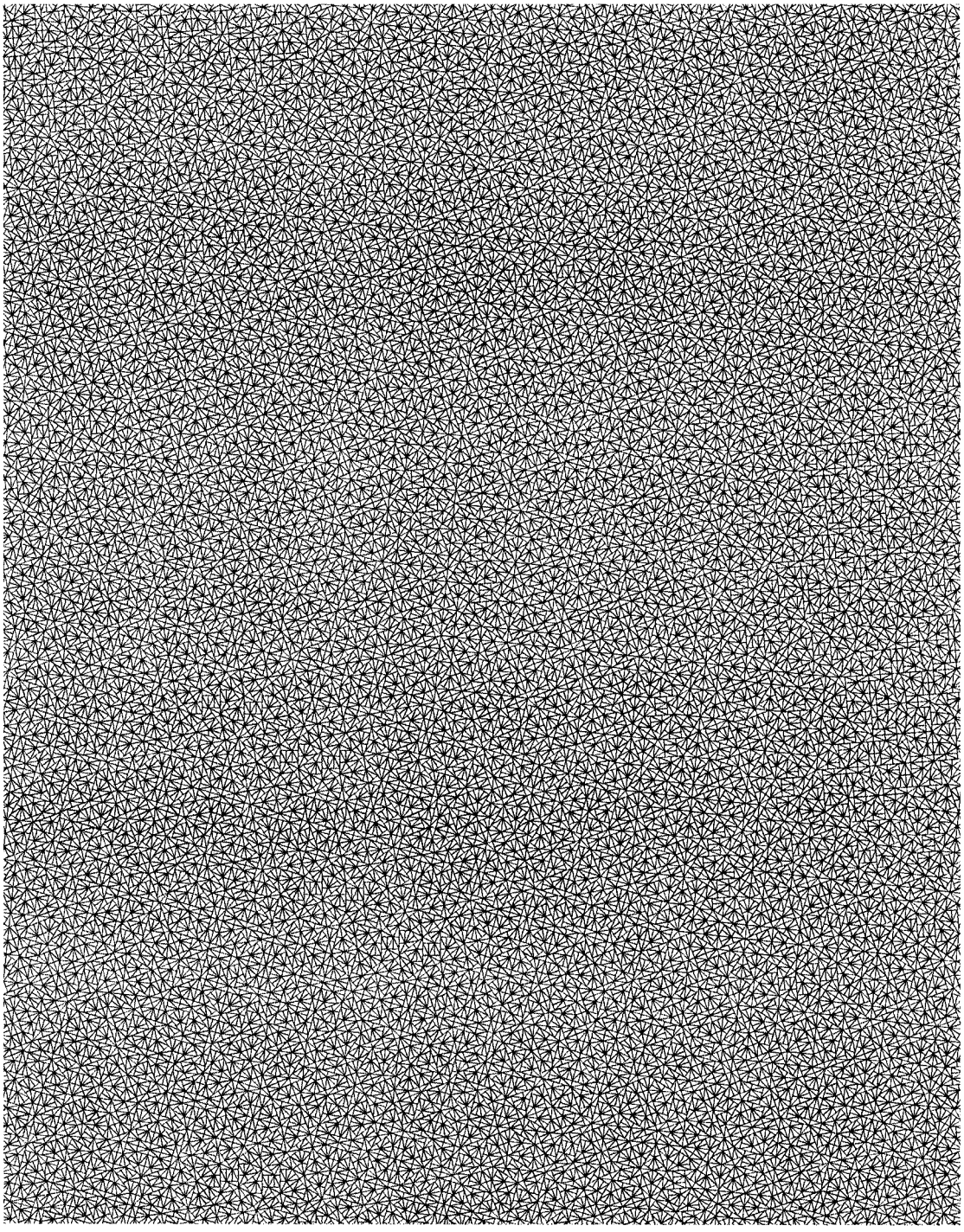

Figure 3: A patch of pinwheel, seven iterations

Chapter 2 - Pinwheel Preliminaries

2.1 Conventions and Definitions

When dealing with an object as complicated as the pinwheel tiling, it is essential to be extremely careful and explicit in the setup phase of the investigation. We initiate this process with an important convention: for convenience of calculation, we will consider all points as elements of the complex plane $\mathbb{C}$ for the remainder of the thesis. However, at all times, we must bear in mind that the pinwheel tiling is actually an object residing in $\mathbb{R}^2$.

Definition 2.1 *By a* **pinwheel tile**, *we mean a* $2 : 4 : 2\sqrt{5}$ *right triangle (we double the lengths of the sides for convenience in coordinatization). We will use the terms* **short leg, long leg, and hypotenuse** *in the obvious manner to refer to the various sides of the triangle.*

Definition 2.2 *An object is said to be* **chiral** *if its reflected image cannot be exactly superimposed over the original. Equivalently, an object is chiral if it possesses no planes of mirror symmetry.*

Note that the $2 : 4 : 2\sqrt{5}$ right triangle is chiral.

Definition 2.3 *Let* Γ_0 *be the* $2 : 4 : 2\sqrt{5}$ *right triangle with vertices* $-1-i$, $1-i$, *and* $-1+3i$. *We will say that a triangle congruent to* Γ_0 *has* **positive chirality** *(or is a* white *triangle, or is* type 1 *for matrix indexing purposes) if it can be superimposed on* Γ_0 *by a Euclidean motion (a series of translations and rotations, conceptually equivalent to freely sliding the triangle around in the plane). Any triangle congruent to* Γ_0 *that cannot be superimposed over* Γ_0 *by a Euclidean motion is said to have* **negative chirality** *(or is a* gray *triangle, or is* type 2 *for matrix indexing purposes).*

Definition 2.4 *The* **pinwheel tiling** *is obtained by iteratively applying the substitution seen in Figure 2 to* Γ_0 *infinitely many times. We shall denote the pinwheel tiling by* Γ. Γ_n *denotes the set of* 5^n *tiles obtained by iterating the substitution n times; we shall refer to all such sets of tiles as* **iterates** *of the pinwheel tiling.* $\partial\Gamma_n$ *will be used to refer to the triangular outer perimeter of each iterate.*

We will arrive at a coordinatized version of the pinwheel substitution later. At that time, it will be clear why we begin with this specific positive chiral triangle.

Definition 2.5 $U(1) := \{x \mid x \in \mathbb{C}, |x| = 1\}$ *is the group of rotations around 0 in the plane.*

Definition 2.6 $\omega := -\arctan(\frac{1}{2})$. $\theta_\omega := e^{\omega i} \in U(1)$ *is the rotation through* ω. *In general,* $\theta_\alpha := e^{\alpha i}$ *is the rotation through the angle* α.

Definition 2.7 *Let* γ *be any tile in* Γ. *Let* x *be the vertex at the right angle of* γ *and let* y *be the other terminal vertex of the short leg. Let* θ *be* $\frac{1}{2}(y - x)$. *We define the* **orientation** *of* γ *to be* $\theta \in U(1)$.

2.2 Tile - Control Point Equivalence

Generally speaking, it is more convenient to work with points than with triangles. Rather than using the vertices of the tiles, we instead follow Radin's work to a more efficient set of distinguished points.

Proposition 2.8 *The point* $0 + 0i$ *has the same relative position within each iterate of the pinwheel tiling.*

Proof: Suppose that the point $x + iy$ has the same relative position within each iterate of the pinwheel tiling. Because the rotation component of the substitution must occur about this point, we will henceforth call it the **hub** of the pinwheel tiling. The location of the hub is found using the fact that $\partial\Gamma_0$ and $\partial\Gamma_1$ are coordinatized similar triangles.

From the similar triangles in Figure 4, we get the following system of equations:

$$\begin{aligned} 5((x+1)^2 + (y+1)^2) &= (x+3)^2 + (y+1)^2 \\ 5((x+1)^2 + (y-3)^2) &= (x-1)^2 + (y-7)^2 \\ 5((x-1)^2 + (y+1)^2) &= (x-1)^2 + (y+3)^2 , \end{aligned}$$

which simplifies to

$$\begin{aligned} 4x^2 + 4y^2 &= -4x - 8y \\ 4x^2 + 4y^2 &= -12x + 16y \\ 4x^2 + 4y^2 &= 8x - 4y . \end{aligned}$$

Solving this system gives the desired result. □

Note that we coordinatized Γ_0 with the intent of making the hub and the origin coincide.

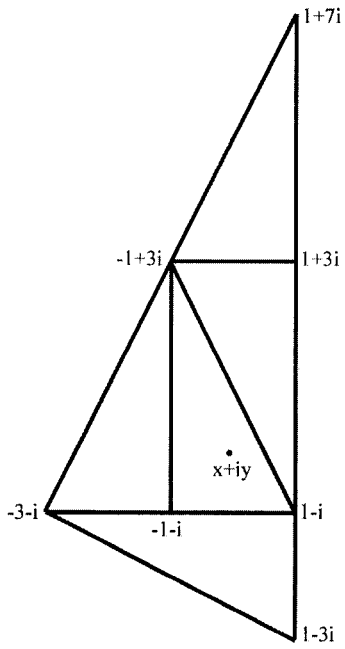

Figure 4: Locating the hub

Definition 2.9 *Let γ be any tile in Γ. The* **control point** *of γ is a triple (x, θ_α, χ) consisting of the location of the analogue of hub inside γ, the orientation of γ, and the chirality of γ respectively. The set of all control points in Γ is denoted by Λ and the set of the control points of Γ_n is Λ_n. By Λ^+, Λ^- we mean the subsets of Λ comprised of the control points of positive and negative chirality, respectively.*

For convenience, we will frequently relax this definition slightly and refer to the location component alone as a control point. However, we must always remember that control points must consist of three pieces of information for the following essential result to hold true:

Proposition 2.10 *Γ and Λ are mutually locally derivable.*

Proof: This is equivalent to saying that, given any pinwheel tile we can find its control point and given any control point (including orientation and chirality), we can find the locations of the vertices of its associated tile using only local information. Let $x, y, z \in \mathbb{C}$ be the vertices at the right, large, and small angles of a pinwheel tile respectively. Then the location of the control point is $\frac{x+2y+z}{4}$, the orientation is $\frac{1}{2}(y-x)$, and the chirality is obvious by inspection. Conversely, suppose a control

point is given by (w, θ_α, χ). Then the vertices of its associated tile are given by $w + (\theta_\alpha + \theta_{\alpha - \chi\frac{\pi}{2}})$, $w + (\theta_{\alpha+\pi} + \theta_{\alpha-\chi\frac{\pi}{2}})$, and $w + (\theta_{\alpha+\pi} + 3\theta_{\alpha+\chi\frac{\pi}{2}})$. □

Thanks to this result, we will now work almost exclusively with the control points.

Our next goal is to use the equivalence between Γ and Λ to translate our geometric representation of the pinwheel substitution into a formula.

Definition 2.11 *The* **Euclidean Motion Group** $E(2) = U(1) \ltimes \mathbb{R}^2$ *is the group of all planar transformations that consist of translations and rotations. We will consider the following representation:*

$$E(2) := \left\{ \begin{pmatrix} \theta_\alpha & x \\ 0 & 1 \end{pmatrix} \middle| \, \theta_\alpha \in U(1), x \in \mathbb{C} \right\}.$$

So we can consider each element of Λ to be a pair consisting of an element of $E(2)$ and ± 1, representing chirality. We can now write a formula for the pinwheel substitution on the control points.

Definition 2.12 *The* **pinwheel substitution** *is given by:*

$$\left(\begin{pmatrix} \theta_\alpha & x \\ 0 & 1 \end{pmatrix} \quad \chi \right) \mapsto \begin{cases} \left(\begin{pmatrix} \theta_{\alpha+\omega-\chi\omega} & \sqrt{5}\theta_\omega x \\ 0 & 1 \end{pmatrix} \quad \chi \right) \\ \left(\begin{pmatrix} \theta_{\alpha+\omega-\chi\omega+\pi} & 2\theta_{\alpha+\omega-\chi\omega+\chi\frac{\pi}{2}} + \sqrt{5}\theta_\omega x \\ 0 & 1 \end{pmatrix} \quad \chi \right) \\ \left(\begin{pmatrix} \theta_{\alpha+\omega-\chi\omega+\pi} & 4\theta_{\alpha+\omega-\chi\omega+\chi\frac{\pi}{2}} + \sqrt{5}\theta_\omega x \\ 0 & 1 \end{pmatrix} \quad -\chi \right) \\ \left(\begin{pmatrix} \theta_{\alpha+\omega-\chi\omega+\pi} & 2\theta_{\alpha+\omega-\chi\omega+\pi} + \sqrt{5}\theta_\omega x \\ 0 & 1 \end{pmatrix} \quad -\chi \right) \\ \left(\begin{pmatrix} \theta_{\alpha+\omega-\chi\omega-\chi\frac{\pi}{2}} & 2\theta_{\alpha+\omega-\chi\omega-\chi\frac{\pi}{2}} + \sqrt{5}\theta_\omega x \\ 0 & 1 \end{pmatrix} \quad -\chi \right). \end{cases}$$

Figure 5 shows how we arrived at this substitution:

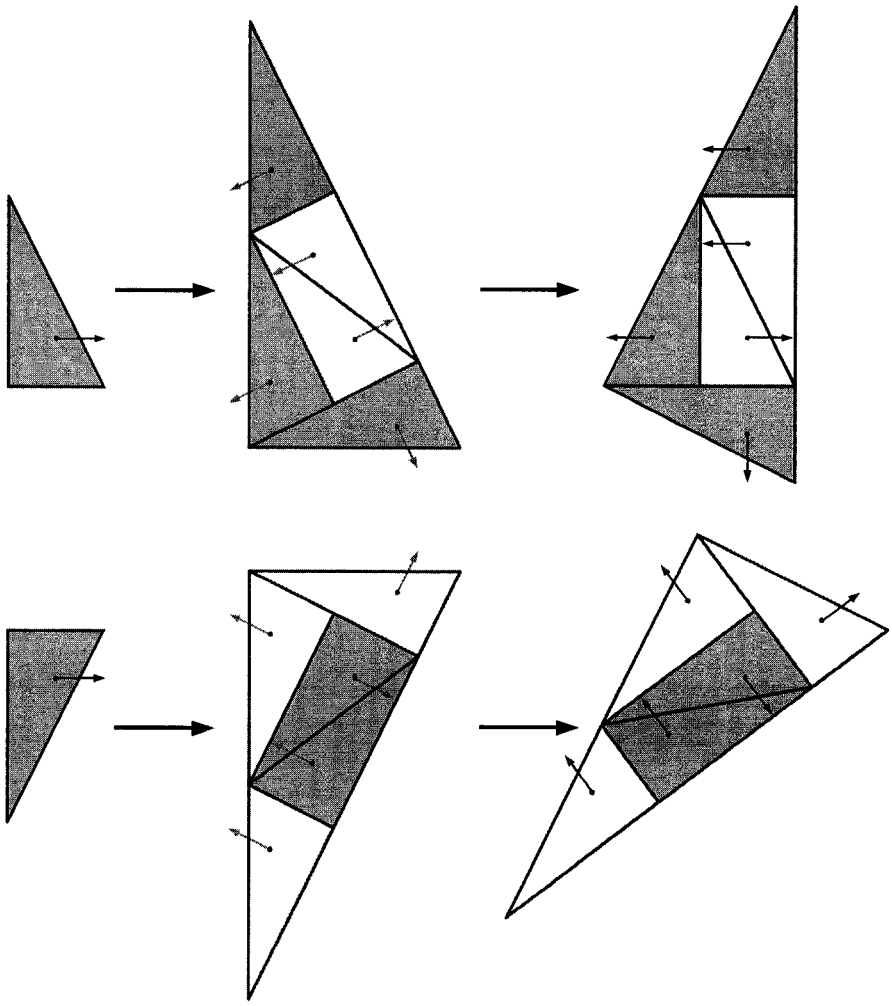

Figure 5: Pinwheel substitution on tiles and points

By superimposing the control points on our geometric interpretation of the substitution, it is easy to see how we derived the substitution formula. We have broken the substitution into two steps: an inflation and subdivision step, and a rotation step. Clearly, the subdivision depends on the chirality of the original triangle. However, and this is a crucial point, the rotation step applies θ_ω to every point *independent* of its chirality. The reason for the rotation step is to ensure the existence of a fixed point by correcting for the rotating effect implicit in the subdivision, and hence the direction of the corrective rotation depends entirely on the chirality of the starting point Λ_0.

By infinitely iterating the above substitution on the set starting with the single element

$$\Lambda_0 = \left(\begin{pmatrix} \theta_0 & 0 \\ 0 & 1 \end{pmatrix} \quad 1 \right)$$

we generate Λ. Note that we arbitrarily started with a tile of positive chirality; we could just as easily have used a negative chirality tile. If we repeated the above arguments for this case, we would obtain a tiling that is a mirror image of the pinwheel tiling. This process would also involve the creation of a mirror substitution. We will use the iterates of this mirror tiling in Chapter 4.

Definition 2.13 *$V_n := \overline{\Lambda_n}$ is the nth iterate of the mirror pinwheel tiling.*

2.3 Two Chiralities, Infinite Orientations

Proposition 2.14 *ω is irrational with respect to π.*

Proof (by contradiction): Let $\mathbb{A}$ denote the ring of algebraic integers (the set of all roots of monic polynomials in $\mathbb{Z}[X]$). Suppose ω is rational with respect to π. Then $\exists\, a, n \in \mathbb{Z}$ such that $\omega = \frac{a}{n}\pi$, i.e. $n\omega = a\pi$. Hence, $e^{in\omega} = e^{ia\pi} = \pm 1$. Let $\alpha = e^{i\omega}$. Then $\alpha^n = \pm 1$ so $\alpha, \overline{\alpha} \in \mathbb{A}$ since they are roots of the polynomial $X^n \mp 1$. It follows that $\alpha + \overline{\alpha} = 2\cos\omega \in \mathbb{A}$, so $(2\cos\omega)^2 \in \mathbb{A}$. But $(2\cos\omega)^2 = (2(\frac{2}{\sqrt{5}}))^2 = \frac{16}{5} \in \mathbb{Q}$. Therefore $\frac{16}{5} = (2\cos\omega)^2 \in \mathbb{A} \cap \mathbb{Q} = \mathbb{Z}$, which is a contradiction. The desired result follows. □

When combined with the pinwheel substitution, Proposition 2.14 shows us that the pinwheel tiles occur in infinitely many orientations, and this is arguably the most significant property of the tiling. We shall examine the orientations in greater detail in Chapter 3.

We are finally in a position to provide a straightforward proof of the aperiodicity of Λ, and therefore Γ:

Proposition 2.15 *Λ is an aperiodic tiling.*

Proof (by contradiction): First, we observe that if Λ is periodic in one direction, then it is periodic (that is, that there exists two independent translations mapping Λ onto itself). To see this, suppose that $t + \Lambda = \Lambda$ for some $t \in \mathbb{C}$. Then, because any pattern observed among the individual points is echoed in the arrangement of the copies of Λ_1, we have that $\sqrt{5}\theta_\omega t + \Lambda = \Lambda$.

Now, assume for a contradiction that Λ is periodic. Then, by definition, there exist $s, t \in \mathbb{C}$ independent such that $s + \Lambda = \Lambda$ and $t + \Lambda = \Lambda$. Hence, there exists a finite fundamental region T with $\bigcup_{m,n\in\mathbb{Z}} ms + nt + T = \Lambda$. But then, every point in Λ must have the same orientation as some point in T. Since we know Λ exhibits infinitely many orientations, this is a contradiction. Therefore, Λ is aperiodic. □

Putting orientations aside for the moment, we now prove a preliminary result about the chiralities.

Proposition 2.16 *$m_k := \frac{5^k+(-1)^k}{2}$, $n_k := \frac{5^k-(-1)^k}{2}$ are the number of chirality 1, -1 points in Λ_k respectively.*

Proof (by induction):
$k = 0$:

$$m_0 = \frac{5^0 + (-1)^0}{2} = \frac{1+1}{2} = 1;\ n_0 = \frac{5^0 - (-1)^0}{2} = \frac{1-1}{2} = 0\,.$$

Induction step:

$$\begin{aligned} m_{k+1} &= 2m_k + 3n_k = \frac{1}{2}(2\cdot 5^k + 2(-1)^k + 3\cdot 5^k - 3(-1)^k) \\ &= \frac{1}{2}(5\cdot 5^k - 1(-1)^k) = \frac{5^{k+1} + (-1)^{k+1}}{2}\,; \\ n_{k+1} &= 3m_k + 2n_k = \frac{1}{2}(3\cdot 5^k + 3(-1)^k + 2\cdot 5^k - 2(-1)^k) \\ &= \frac{1}{2}(5\cdot 5^k - (-1)(-1)^k) = \frac{5^{k+1} - (-1)^{k+1}}{2}\,. \end{aligned}$$

□

From Proposition 2.16, we can see that Λ consists of tiles of positive and negative chirality in equal proportion. This result helps motivate the next section.

2.4 Mutual Local Derivability of Chiralities

Theorem 2.17 *Λ^+ and Λ^- are mutually locally derivable.*

Proof: This is equivalent to saying that given Λ^+, all of Λ^- is uniquely forced by local rules and vice versa. We will start with Λ^+, but the argument in the other direction is identical. First, we move from Λ^+ to Γ^+ using Proposition 2.10. So we start off with the plane filled with tiles of positive chirality with gaps between them. Our task then is to show that the gaps are uniquely fillable by tiles of negative chirality. The introduction of some terminology will prove beneficial at this point. We say that two tiles **abut** if they meet along an edge (as opposed to only at a vertex or not at all).

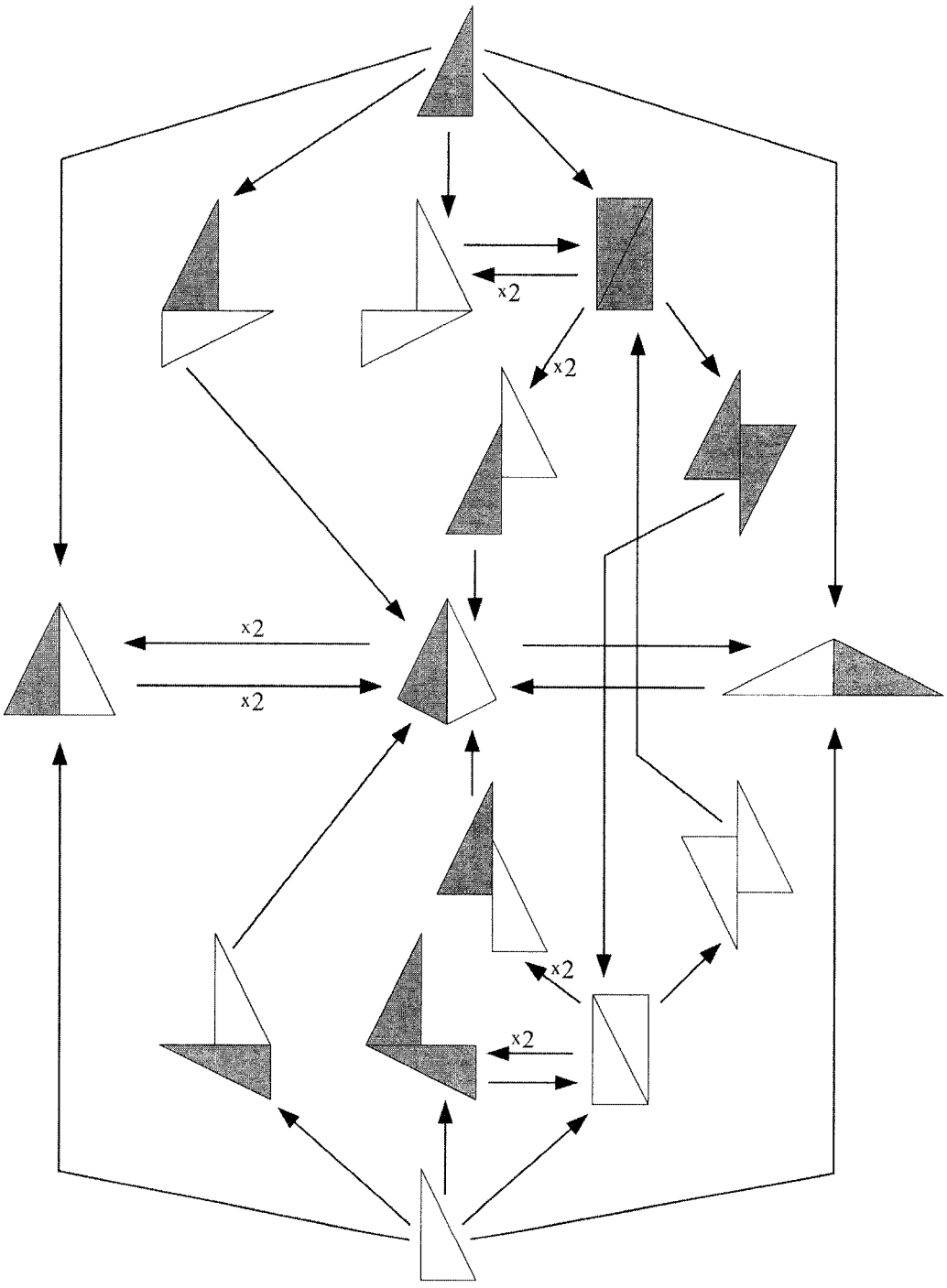

Figure 6: Abutment atlas for the pinwheel tiling

An edge is **valent** if it does not abut any other edge. An edge is **full** if it abuts other edges for its entire length.

The first step in this proof is to describe every way in which two tiles may abut legally in the pinwheel tiling. The easiest way to do this is to apply the substitution to a single tile of positive chirality, record every type of abutment that occurs in the result, then apply the substitution to each pair of abutting tiles. Continue this process until no new abutment types result. Repeat, this time starting with a tile of negative chirality. By following this process to its conclusion, I have arrived at the 'abutment atlas' seen in Figure 6. It is a comprehensive diagram of all legal abutments in the pinwheel tiling. The $\times 2$ situated by certain arrows in the atlas signify that two copies of the resultant configuration arise from applying the pinwheel substitution to the antecedent configuration.

With the abutment atlas to guide us, we obtain a very nice algorithm for filling the gaps uniquely. Note that the algorithm itself is not unique; the uniqueness of tile placement comes directly from the valences observed in Γ^+:

(i) Abut the long edge of a gray tile to every valent long edge in Γ^+, resulting in a new set of extant tiles Γ'. Note that there is one and only one way to fully abut the long edges of a white tile and a gray tile, and that there is no other way to legally fill a valent long white edge with only gray edge abutments.

(ii) Abut the hypotenuse of a gray tile to every valent hypotenuse in Γ', thereby creating Γ''. The abutment atlas shows that a hypotenuse may only fully abut another hypotenuse, and there is a simple reason why this is the case: the hypotenuse of a pinwheel tile has irrational length, and the other two legs have integer lengths! Since all white tiles are already placed, it immediately follows that these abutments are unique and are required to complete our task of filling the gaps.

(iii) Consider the remaining gaps. We know there must be at least one way to fill them, namely $\Gamma \setminus \Gamma''$. Let Δ be an arbitrary set of tiles that fill the remaining gaps. What remains to be shown is that Δ is unique. It is an easy – if somewhat tedious – process to accomplish this by considering the restrictions imposed by the abutment atlas on the configurations of gray tiles allowed in Δ. First, consider that every $\delta \in \Delta$ must abut hypotenuses with another tile in Δ because no valent hypotenuses remain in Γ'' following step (ii). Hence, Δ must be composed entirely of rectangles consisting of two gray tiles. Furthermore, by step (i), we know that none of these rectangles may fully abut long edges with

a white tile. From the abutment atlas, we see there are exactly three configurations that give rise to a gray rectangle. However, there is only one configuration of tiles that yields a gray rectangle that can be in Δ: Configuration IV (in Figure 7). In each of Configurations I, II, and III, the gray rectangle abuts long edges with a white tile. It is significant to note at this point that Configuration IV is observed to occur in the third iterate of the pinwheel tiling and hence Δ consists of infinitely many gray rectangles. We now examine how the rectangles of Δ may abut each other; we are still concerned about finding a configuration that does not fill a gap uniquely (for example, a square gap filled with two vertical gray rectangles could also potentially be filled with two horizontal gray rectangles). Given that each gray rectangle in Δ must be accompanied by the entirety of Configuration IV, the interaction possibilities are severely limited. First, we note that tile A of Configuration IV is in Γ'' because it abuts long edges with a white tile.

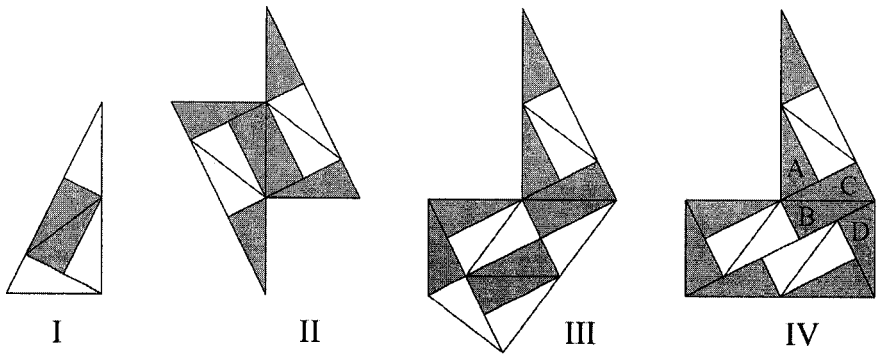

Figure 7: Local Configurations 1

B and C are in Δ, while D could be in either Γ'' or Δ with the given information. We note that the abutments seen in Figure 8 do not occur in the abutment atlas and hence are illegal:

We now see there are three possible abutment scenarios given:

(a) Tile D is in Γ'' and the tile that abuts the short side of tile C is also in Γ''; hence, the underlying gap consists of an isolated rectangle.

(b) Either tile D is in Δ (Configuration V in Figure 9) or the tile that abuts the short side of tile C is in Δ (Configuration VI) but not both. Configuration V and VI are equivalent: they both consist of two overlapping copies of

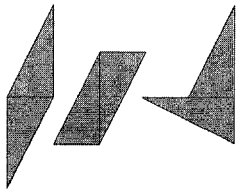

Figure 8: Three illegal abutments

Configuration IV, and can be seen to vary only by a rotation through 90 degrees and their labeling. Note that, in both Configuration V and VI, one lettered tile belongs to both copies of Configuration IV and hence ends up with two labels. Configuration V comes immediately because D is in Δ and hence must be surrounded by Configuration IV. The abutment to the short leg of C observed in Configuration VI is the only legal possibility. If $D' \in \Delta$ or the tile abutting C^* is in Δ, then part (c) below shows that we arrive at a contradiction. Therefore, the underlying gap in both cases consists of an isolated L shape.

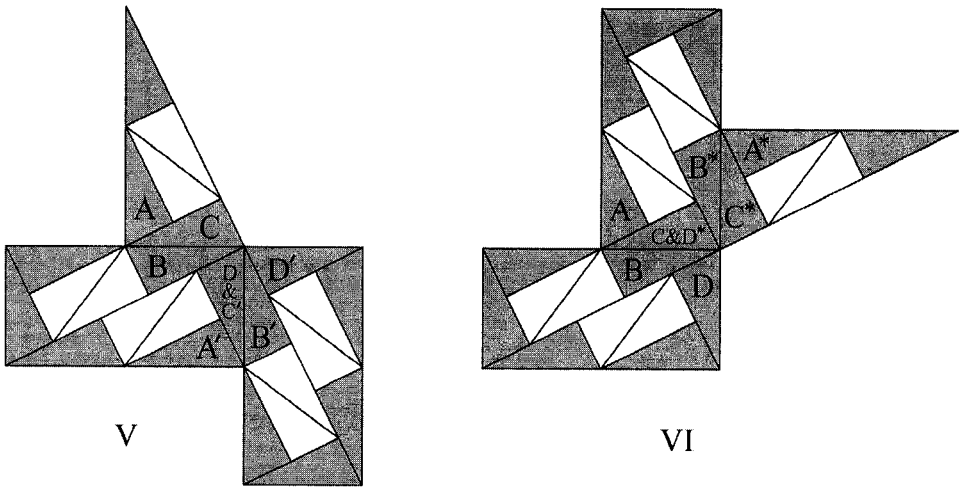

Figure 9: Local Configurations 2

(c) Both tile D and the tile abutting the short side of tile C are in Δ. As we see from Configuration VII in Figure 10, this creates a situation which forces Configuration VIII (this follows from the fact that tiles may not overlap, and from the severe restrictions on hypotenuse abutment). Hence, a gap consisting of exactly three rectangles is impossible.

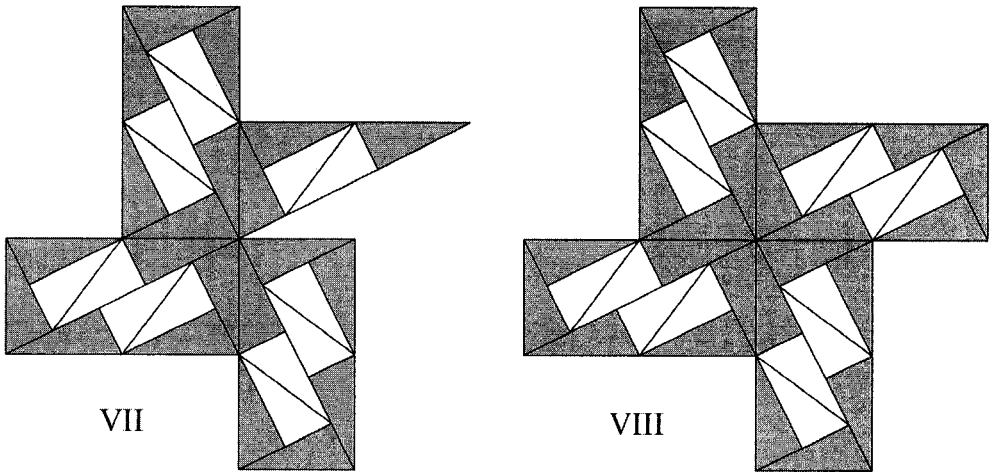

Figure 10: Local Configurations 3

In each of the three above cases, we have no remaining valences that allow for more Δ rectangle abutments, and hence the list is complete. Hence, we have shown that the gaps remaining in Γ'' may occur in one of three finite, isolated configurations (we have made no claims that all of these gap types must occur, only that they are possible according to the abutment atlas). But it is immediate that each of these three different gaps can be tiled by gray tiles in one and only one way. Hence, Δ is unique. $\square$

This result, while new and interesting, is not used in the following analysis. It may be of particular interest to anyone attempting to calculate the noncommutative autocorrelation of the pinwheel tiling, as suggested in Chapter 5. As we draw our preliminary findings to a close and begin on said analysis, a final remark about Λ is appropriate. The sequence $\{\Lambda_n\}_n$ exhibits exponential growth in the number of control points observed, but only linear growth in the number of orientations. This proves to be an interesting computational obstacle.

Chapter 3 - Orientations

The infinite tile orientations exhibited in the pinwheel tiling comprise its salient feature. We therefore begin our analysis of the tiling by examining this property. We first develop a recursive algorithm that allows us to observe how the orientations accumulate.

Lemma 3.1 *Let* v *be a vector that makes the angle* α *with the positive x-axis. Let* A *be a line through the origin which makes the angle* β *with the positive x-axis. Suppose* v′ *is the reflection of* v *in* A. *Then* v′ *makes the angle* $2\beta - \alpha$ *with the positive x-axis.*

Proof: The following diagram illustrates the situation when $\beta > \alpha$ (the picture when $\beta < \alpha$ is very similar):

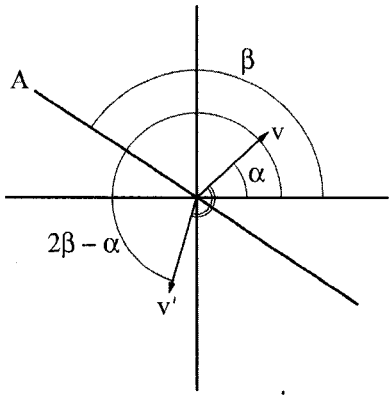

Figure 11: Illustration of Lemma 3.1 for $\beta > \alpha$

By symmetry, the angle between v and A is congruent with the angle between v′ and A and both have measure $\beta - \alpha$. The desired result follows by angle addition. □

Suppose $\lambda \in \Lambda_n$ has orientation and chirality (θ_α, χ). After applying the substitution to Λ_n, we obtain Λ_{n+1}, and λ spawns five points. The question at hand is, what are the orientation and chirality of those five points? One of the points is obvious: one branch of the substitution is the identity map and hence we obtain (θ_α, χ). It also immediately follows from the substitution that one of the points will lie in a copy of Λ_n that has simply been rotated through π; this point has orientation and chirality $(\theta_{\alpha+\pi}, \chi)$.

From the substitution, it is clear that the third and fourth points are identical up to translation. As seen in Figure 5, the third point will be a reflection of λ in the

line coincident with the long leg of Γ_n. Since the orientation of Γ_n is $n\omega$, this line makes the angle $\frac{\pi}{2} + n\omega$ with the positive x-axis. Applying Lemma 3.1, we get that the orientation and chirality of points three and four is $(\theta_{\pi+2n\omega-\alpha}, -\chi)$. The fifth point differs from the previous two only in a rotation through $\frac{\pi}{2}$, and hence we get $(\theta_{\frac{3\pi}{2}+2n\omega-\alpha}, -\chi)$.

It immediately follows from the substitution that every orientation observed in the pinwheel tiling can be written in the form $a\frac{\pi}{2} + 2m\omega$, where $a \in \{0, 1, 2, 3\}$ and $m \in \mathbb{N}$. Furthermore, we can say that if a point λ is found in Λ_n then its orientation has $0 \leq m \leq n-1$. We have essentially proven the following:

Proposition 3.2 *Let* $h : \mathbb{Z}_+ \times \mathbb{Z}_+ \times \mathbb{Z}/4\mathbb{Z} \times \{-1, 1\}$ *be defined recursively by:*
$h(0, 0, 0, 1) = 1$;
$h(0, m, a, \epsilon) = 0$ *for all* $(m, a, \epsilon) \neq (0, 0, 1)$;
$h(n+1, m, a, \epsilon) =$

$$h(n, m, a, \epsilon) + h(n, m, a+2, \epsilon) + 2h(n, n-m, 2-a, -\epsilon) + h(n, n-m, 3-a, -\epsilon).$$

Then $h(n, m, a, \epsilon)$ *is the number of points with orientation and chirality* $(a\frac{\pi}{2} + 2m\omega, \epsilon)$ *inside* Λ_n.

It is useful to note that because $0 \leq m \leq n-1$, $a \in \mathbb{Z}/4\mathbb{Z}$, and $\epsilon \in \{-1, 1\}$, the number of different orientation and chirality pairs observed in Λ_n will be between n and $8n$.

Figure 12 plots $a\frac{\pi}{2} + 2m\omega$ vs $\epsilon \cdot \frac{h(n,m,a,\epsilon)}{5^n}$ for select n. These graphs suggest that the orientations observed in Λ are uniformly distributed. Proving this is the focus of our next section.

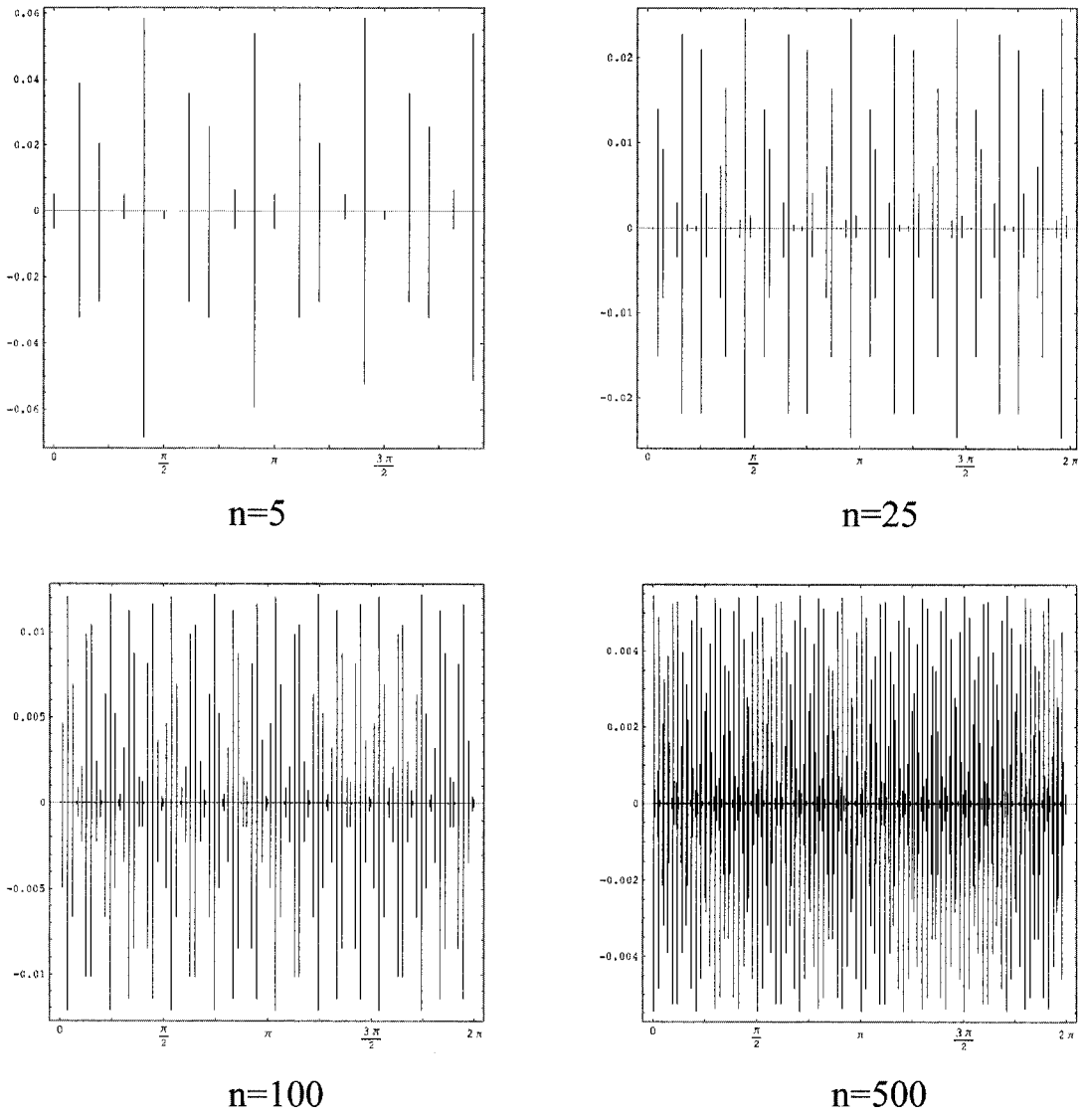

Figure 12: Angle distributions in four pinwheel iterates

3.1 Uniform Distribution of Orientations

Radin has previously demonstrated in [12] that the orientations of the pinwheel tiles are uniformly distributed. We supply a similar proof with more details. The following definition depends on the fact that there is an exact copy of Λ_k in Λ_{k+1}:

Definition 3.3 *Let $\{\alpha_i\}_{i=1}^{\infty}, \{\beta_i\}_{i=1}^{\infty} \subseteq [0, 2\pi)$ be two sequences of angles such that for any k, $\theta_{\alpha_1}, \ldots, \theta_{\alpha_{m_k}}$ are the orientations of the $\chi = 1$ points in Λ_k and $\theta_{\beta_1}, \ldots, \theta_{\beta_{n_k}}$ are the orientations of the $\chi = -1$ points.*

Definition 3.4 $\{z_n\}_{n=1}^{\infty} \subset U(1)$ *is* **uniformly distributed on** $U(1)$ *if*

$$\lim_{N\to\infty} \frac{1}{N} \sum_{n=1}^{N} f(z_n) = \int_{U(1)} f(z) d\lambda^{U(1)}(z) = \lambda^{U(1)}(f)$$

for all $f : U(1) \to \mathbb{C}$ continuous ($\lambda^{U(1)}$ is defined in Definition 4.9).

Definition 3.5 $\{\gamma_j\}_{j=1}^{\infty} \subset [0, 2\pi)$ *is* **uniformly distributed modulo** 2π *if* $\{e^{i\gamma_j}\}_{j=1}^{\infty}$ *is uniformly distributed on* $U(1)$.

Some preliminary material must be established before we prove the desired result:

Theorem 3.6 (Weyl Criterion) $\{z_n\}_{n=1}^{\infty} \subset U(1)$ *is uniformly distributed if and only if* $\forall\, t \in \mathbb{Z} \setminus \{0\}$ *we have*

$$\lim_{N\to\infty} \frac{1}{N} \sum_{n=1}^{N} (z_n)^t = 0\,.$$

Proof: ($\Longleftarrow$) Suppose that $\lim_{N\to\infty} \frac{1}{N} \sum_{n=1}^{N} z_n^t = 0$ for all non-zero integers t. Let $f : U(1) \longrightarrow \mathbb{C}$, and suppose at first that it is representable (that is, it is uniformly represented by its Fourier series):

$$f(z) = \sum_{t=-\infty}^{\infty} a_t z^t\,, \quad \text{where } a_t = \int_{U(1)} f(z) z^{-t} d\lambda^{U(1)}(z)\,.$$

Choose any $\epsilon > 0$ and then $M > 0$ so that

$$\left| f(z) - \sum_{|t|\le M} a_t z^t \right| < \epsilon$$

for all $z \in U(1)$. Then for all $N > 0$,

$$\left| \frac{1}{N} \sum_{n=1}^{N} f(z_n) - \sum_{|t| \leq M} a_t \frac{1}{N} \sum_{n=1}^{N} z_n^t \right| = \left| \frac{1}{N} \sum_{n=1}^{N} f(z_n) - \frac{1}{N} \sum_{n=1}^{N} \sum_{|t| \leq M} a_t z_n^t \right| < \epsilon \,.$$

In view of our assumption on the sequence $\{z_n\}_n$, the averages inside the sum of the left side of this equality are going to 0 with large N, except possibly when $t = 0$. Thus for all $N >> 0$,

$$\left| \frac{1}{N} \sum_{n=1}^{N} f(z_n) - a_0 \right| \leq 2\epsilon \,.$$

Since ϵ was arbitrary and $a_0 = \int_{U(1)} f(z) d\lambda^{U(1)}(z)$, we are done.

Now, in general f need not be representable. However, for all $\epsilon > 0$ there exist representable functions $g = g_\epsilon$ with $||g - f||_\infty < \epsilon$ ([18], Chapter 1, Theorem 3.5). For such a g we have

- $\left| \int_{U(1)} g d\lambda^{U(1)} - \int_{U(1)} f d\lambda^{U(1)} \right| < \epsilon$
- $\left| \frac{1}{N} \sum_{n=1}^{N} g(z_n) - \frac{1}{N} \sum_{n=1}^{N} f(z_n) \right| < \epsilon$
- $\left| \int_{U(1)} g d\lambda^{U(1)} - \frac{1}{N} \sum_{n=1}^{N} g(z_n) \right| < \epsilon, \text{ if } N >> 0 \,.$

These give us

$$\left| \int f d\lambda^{U(1)} - \frac{1}{N} \sum_{n=1}^{N} f(z_n) \right| < 3\epsilon \,,$$

as required.

($\Longrightarrow$) In the reverse direction, assuming that the averaged sums converge to the integrals for continuous functions, we may use the functions $f_t : z \mapsto z^t$ to obtain

$$\lim_{N \to \infty} \frac{1}{N} \sum_{n=1}^{N} z_n^t = \int_{U(1)} z^t d\lambda^{U(1)}(z) \,,$$

which is 0 if $t \neq 0$. □

Definition 3.7 *For any $t \in \mathbb{Z}$, we define*

$$M(t) := \begin{pmatrix} e^{it0} + e^{it\pi} & 2e^{it(2\omega - \pi)} + e^{it(2\omega + \frac{\pi}{2})} \\ 2e^{it(\pi)} + e^{it(-\frac{\pi}{2})} & e^{it(2\omega)} + e^{it(2\omega - \pi)} \end{pmatrix} .$$

Remarks:

(i) This matrix encapsulates the orientational component of the pinwheel substitution. That is, $(M(1))_{jk}$ is the sum of the orientations of the type j tiles obtained after applying the pinwheel substitution to a single type k tile with orientation 1; $(M(t))_{jk}$ simply raises each orientation in the sum to the exponent t, setting us up to use the Weyl Criterion.

(ii) We write e^{it0}, rather than simplifying this expression to 1, because it makes the arguments easier to follow.

(iii) This matrix is similar to the matrix used by Charles Radin in his proof. The primary difference comes from the fact that Radin rotates Λ_n at every step so that, considered as one big triangle, it has orientation θ_0. We must use the above matrix in place of Radin's because of our requirement that we work with a fixed point substitution. Also, Radin's type 1 tile corresponds to what we have chosen to be our type 2 tile and vise versa.

Lemma 3.8 (Radin)

$$(M(t))^k = \begin{pmatrix} \sum_{j=1}^{m_k} e^{it\alpha_j} & \sum_{j=1}^{n_k} e^{it(2k\omega-\beta_j)} \\ \sum_{j=1}^{n_k} e^{it\beta_j} & \sum_{j=1}^{m_k} e^{it(2k\omega-\alpha_j)} \end{pmatrix}$$

Proof: Immediate from Definitions 3.7 and 2.12. □

Since $\lim_{k\to\infty} \frac{m_k}{5^k} = \lim_{k\to\infty} \frac{n_k}{5^k} = \frac{1}{2}$, to prove that $\{\alpha_n\}_n$ and $\{\beta_n\}_n$ are uniformly distributed, it is enough to prove that, $\forall t \neq 0, 1 \leq i, j \leq 2$

$$\lim_{k\to\infty} \frac{((M(t))^k)_{ij}}{5^k} = 0$$

by Theorem 3.6.

Any consideration of matrices associated with substitution tilings will almost invariably utilize the powerful Perron Frobenius theorem, and this thesis is no exception. We state the theorem below; for a proof and further details, see [16].

Definition 3.9 *A square non-negative matrix T is* **primitive** *if there exists $k \in \mathbb{N}$ such that $T^k > 0$.*

Theorem 3.10 (Perron-Frobenius Theorem) *Suppose T is an $n \times n$ non-negative primitive matrix. Then there exists an eigenvalue λ such that:*

(i) $\lambda \in \mathbb{R}, \lambda > 0$;

(ii) λ *can be associated with strictly positive left and right eigenvectors. Moreover, these eigenvectors are unique up to constant multiplication.*

(iii) $\lambda > |\kappa|$ *for any eigenvalue* $\kappa \neq \lambda$;

(iv) If $0 \leq B \leq T$ *and* β *is an eigenvalue of* B, *then* $|\beta| \leq \lambda$. *Moreover,* $|\beta| = \lambda$ *implies* $B = T$.

(v) λ *is a simple root of the characteristic equation of* T.

Lemma 3.11 *Let $A \geq 0$ be a non-negative primitive matrix and let λ be its Perron-Frobenius* (PF) *eigenvalue. Then, $\exists$ constant $c > 0$ such that $\forall\, n > 0$, $\frac{(A^n)_{ij}}{\lambda^n} \leq c$.*

Proof: Let x be a right PF eigenvector, and hence $x_i > 0\ \forall\, i$. $A^n x = \lambda^n x$ implies that $\forall\, i, \sum_{k=1}^{m} (A^n)_{ik} x_k = \lambda^n x_i$, which yields $(A^n)_{ik} x_k \leq \lambda^n x_i$ (because $(A^n)_{ik} \geq 0$). Since $x_i > 0\ \forall\, i$, we can find a constant $c \geq \frac{x_i}{x_j}$, $1 \leq i, j \leq m$. Then $\frac{(A^n)_{ik}}{\lambda^n} \leq c\ \forall\, n, i, k$. □

Proposition 3.12 *For any $t \neq 0$ and $1 \leq i, j \leq 2$, we have*

$$\lim_{k \to \infty} \frac{((M(t))^k)_{ij}}{5^k} = 0$$

Proof: Let $t \neq 0$ be arbitrary but fixed. Let A be the matrix defined by $A_{ij} = |(M(t))_{ij}|$. Then $0 < A \leq \begin{pmatrix} 2 & 3 \\ 3 & 2 \end{pmatrix}$ in an entrywise sense, with the additional restriction $A \neq \begin{pmatrix} 2 & 3 \\ 3 & 2 \end{pmatrix}$. Also $|((M(t))^k)_{ij}| \leq (A^k)_{ij}\ \forall\, k, i, j$. Let λ be the PF eigenvalue of A. Then $\lambda < 5$, since 5 is the PF eigenvalue of $\begin{pmatrix} 2 & 3 \\ 3 & 2 \end{pmatrix}$ (Theorem 3.10, part (iv)). Let c be the constant obtained by Lemma 3.11. Then

$$\left| \frac{((M(t))^k)_{ij}}{5^k} \right| \leq \frac{(A^k)_{ij}}{5^k} = \frac{(A^k)_{ij}}{\lambda^k} \cdot \left(\frac{\lambda}{5}\right)^k \leq c \cdot \left(\frac{\lambda}{5}\right)^k \xrightarrow{k \to 0} 0,$$

since $\frac{\lambda}{5} < 1$. Hence, the desired result follows. □

While the uniform distribution of orientations in the pinwheel tiling may have many interesting consequences, we are only concerned with the effects of this result on its autocorrelation.

Chapter 4 - Autocorrelation of the Pinwheel Tiling

4.1 Introduction to the Autocorrelation

Physical diffraction is a fundamental tool used by materials scientists. It is the most common way of obtaining knowledge about the internal atomic structure of a macroscopic sample. Physical diffraction has a mathematical analogue, and we plan to use mathematical diffraction techniques to probe the structure of the pinwheel tiling. On the path to mathematical diffraction lies an intermediary known as the autocorrelation. As the autocorrelation is a measure, the remainder of the thesis will assume the reader has some background in measure theory; we recommend [4] as a good supplementary measure theory resource. By thoroughly examining the autocorrelation of the pinwheel tiling, we take a significant step towards our goal of understanding this puzzling object.

Throughout this chapter, we will almost exclusively understand Λ to represent only the locations of the control points.

Definition 4.1 $\eta_n := \frac{1}{5^n} \sum_{x,y \in \Lambda_n} \delta_{x-y}$, *the* **averaged autocorrelation** *of* Λ_n. *Here,* δ_z *is the delta measure supported at* $z \in \mathbb{R}^2$.

We note that the volume averaged autocorrelation is the usual object of interest, and that this may be obtained by multiplying the above autocorrelation by $\frac{1}{4}$. Since this multiple has no qualitative impact and serves to clutter our calculations, we prefer to work with η_n.

Definition 4.2 *The vague limit (see Definition 4.8)* $\eta := \frac{1}{4} \lim_{n \to \infty} \eta_n$ *is the averaged autocorrelation of* Λ *(if it exists).*

One of our primary goals for this chapter will be to prove that the autocorrelation does indeed exist.

In defining autocorrelation, one is faced with choosing an averaging sequence, a sequence of compact sets (on which the sums involved are finite) and then taking limits, just as we have done here. In our approach, we are using the sets $\{\Gamma_n\}_n$ for our averaging sequence. For technical reasons, such sequences are chosen to satisfy the van Hove property:

Definition 4.3

(i) For any $A \subset \mathbb{R}^2$ and $K \subset \mathbb{R}^2$ compact, the **K-boundary** *of A is*

$$\partial^K(A) := ((K + A)\backslash A^\circ) \cup ((-K + \overline{\mathbb{R}^2\backslash A}) \cap A),$$

where $^\circ$ and $\overline{\ }$ denote interior and closure, respectively.

(ii) A **van Hove sequence** *is a sequence of compact subsets $\{A_n\}_n \subset \mathbb{R}^d$ such that*

$$\frac{\lambda^{\mathbb{R}^2}(\partial^K(A_n))}{\lambda^{\mathbb{R}^2}(A_n)} \xrightarrow{n\to\infty} 0, \quad \forall\, K \text{ compact}.$$

Proposition 4.4 *$\{\Gamma_n\}_{n=1}^\infty$ is a van Hove sequence.*

Proof: Let $K \subset \mathbb{R}^2$ be compact, and therefore bounded. Hence, $\exists\, r > 0$ so that $K \subset B_r(0)$ and $-K \subset B_r(0)$, where $B_r(0)$ is a closed ball of radius r. Then $\partial^K(\Gamma_n)$ is contained in the set of points of distance $< r$ from the boundary of Γ_n. We know that $\lambda^{\mathbb{R}^2}(\Gamma_n) = 5^n \lambda^{\mathbb{R}^2}(\Gamma_0) = 4 \cdot 5^n$ and the perimeter of $\Gamma_n = (6+2\sqrt{5})5^{\frac{n}{2}}$. Therefore,

$$\frac{\lambda^{\mathbb{R}^2}(\partial^K(\Gamma_n))}{\lambda^{\mathbb{R}^2}(\Gamma_n)} \leq \frac{2r(6+2\sqrt{5})5^{\frac{n}{2}}}{4 \cdot 5^n} \xrightarrow{n\to\infty} 0\,.$$

□

A brief review of a few key measure theoretical concepts will facilitate the arguments in this chapter:

Definition 4.5 *ν is a* **translation bounded** *measure on $(0,\infty)$ if for all $K \subset (0,\infty)$ compact, $\exists\, c > 0$ such that $|\nu(a + K)| < c\ \forall\, a \in (0,\infty)$.*

Definition 4.6 *$\mathcal{M}(\mathbb{R}^2)$ is the space of all regular Borel measures on $\mathbb{R}^2$. $\mathcal{M}^\infty((0,\infty))$ is the space of translation bounded regular Borel measures on $(0,\infty)$.*

Definition 4.7 $\mathcal{K}(\mathbb{R}^2) := \left\{ f : \mathbb{R}^2 \to \mathbb{R} \;\middle|\; f \text{ continuous, } supp(f) \text{ compact} \right\}$.

The Riesz-Markov representation theorem (Theorem 7.2.8 in [4]) establishes a bijection between positive regular Borel measures on $\mathbb{R}^2$ (such as η_n) and continuous linear functionals on $\mathcal{K}(\mathbb{R}^2)$. This map is given by $\mu \mapsto I_\mu$, where $I_\mu(f) := \int f d\mu$. This theorem allows us to define vague convergence, a concept which appeared in the definition of the autocorrelation:

Definition 4.8 *A sequence of measures* $\{\mu_n\}_n \subset \mathcal{M}(\mathbb{R}^2)$ **converges vaguely** *to* $\mu \in \mathcal{M}(\mathbb{R}^2)$ *if, for all* $f \in \mathcal{K}(\mathbb{R}^2)$, $\{\mu_n(f)\}_n \overset{n\to\infty}{\longrightarrow} \mu(f)$.

We adopt the following notation:

Definition 4.9 *We will use* $\lambda^{\mathbb{R}^2}$ *to stand for Lebesgue measure on* $\mathbb{R}^2$, *and* $\lambda^{U(1)}$ *to stand for normalized Haar measure on* $U(1)$ *(we use the superscripts to keep them unequivocally distinct from the various other* λ *seen throughout this thesis).*

4.2 Objectives

In the remainder of this chapter, we are going to examine the autocorrelation of the pinwheel tiling in as much detail as we can. First, we will build a pinwheel substitution formalism for measures. The pinwheel substitution of Definition 2.12 involves complication causing reflections that we would prefer to avoid. To that end, our formalism will work with measures on both Λ_n and V_n, the mirror pinwheel of Definition 2.13. In this case, it will be sufficient to reflect the mirror measures only once at the very end to get them into the correct place. Figure 13 illustrates the formalism in action and will be an extremely valuable reference throughout this chapter. Once we have established our formalism, we will use it to generate the η_n. By letting $n \to \infty$, we demonstrate that the autocorrelation η does exist. In addition to verifying the existence of the autocorrelation, our formalism does give us some structural information. The primary objective of this chapter is to verify that η is circularly symmetric, a fact which depends directly on the uniform distribution result of Chapter 3.

4.3 Substitution Formulation for Measures

Definition 4.10 $\mathcal{P} := \mathbb{C} \setminus \{0\}$, *the punctured complex plane.*

Definition 4.11 *For any* $\alpha \in [0, 2\pi)$, *we can define a map* $R(\alpha) : \mathcal{P} \to \mathcal{P}$ *(rotation through angle* α*) by:*

$$R(\alpha)(z) := e^{i\alpha} z\,.$$

Definition 4.12 $\mathcal{M}^*_{pp}(\mathcal{P}) := \left\{ \sum_{k=1}^n c_k \delta_{a_k} \;\middle|\; c_k \in \mathbb{R}, n \geq 0, a_k \in \mathcal{P} \right\}$, *the span of all real finitely supported measures on* $\mathcal{P}$.

So, $R(\alpha)$ acts naturally on $\mathcal{M}^*_{pp}(\mathcal{P})$: $R(\alpha)(\sum_{k=1}^n c_k \delta_{a_k}) := \sum_{k=1}^n c_k \delta_{R(\alpha)(a_k)}$.

Definition 4.13 *Let* $\Omega, \Phi : (\mathcal{M}^*_{pp}(\mathcal{P}))^2 \to (\mathcal{M}^*_{pp}(\mathcal{P}))^2$ *be linear maps defined by:*

$$\Omega \begin{pmatrix} \mu \\ \nu \end{pmatrix} := \begin{pmatrix} R(-\omega) & 0 \\ 0 & R(\omega) \end{pmatrix} \begin{pmatrix} \mu \\ \nu \end{pmatrix}$$

$$\Phi \begin{pmatrix} \mu \\ \nu \end{pmatrix} := \frac{1}{5} \begin{pmatrix} R(0) + R(\pi) & 2R(\pi) + R(-\frac{\pi}{2}) \\ 2R(-\pi) + R(\frac{\pi}{2}) & R(-0) + R(-\pi) \end{pmatrix} \begin{pmatrix} \mu \\ \nu \end{pmatrix}$$

The maps Ω and Φ compose the core of our desired formalism.

Definition 4.14 *For any* $k \geq h \geq 1$, *define the linear map* $\Psi^k_h : (\mathcal{M}^*_{pp}(\mathcal{P}))^2 \to (\mathcal{M}^*_{pp}(\mathcal{P}))^2$ *by:*

$$\Psi^k_h \begin{pmatrix} \mu \\ \nu \end{pmatrix} := \Omega^{-k}\Phi\Omega^k\Omega^{-(k-1)}\Phi\Omega^{k-1}\ldots\Omega^{-h}\Phi\Omega^h \begin{pmatrix} \mu \\ \nu \end{pmatrix}.$$

If we define Ψ^0_1 to be the identity map, then we have $\Psi^k_h \begin{pmatrix} \mu \\ \nu \end{pmatrix} = \Psi^k_l \Psi^{l-1}_h \begin{pmatrix} \mu \\ \nu \end{pmatrix}$ for $k \geq l \geq h \geq 1$. This decomposition of Ψ^k_h will feature in several induction arguments.

Proposition 4.15 *For any* $k \geq h \geq 1$,

$$\Psi^k_h \begin{pmatrix} \mu \\ \nu \end{pmatrix} = \frac{1}{5^{k-(h-1)}} \begin{pmatrix} \sum_{j=1}^{m_{k-(h-1)}} R(\alpha_j) & \sum_{j=1}^{n_{k-(h-1)}} R(2h\omega + \beta_j) \\ \sum_{j=1}^{n_{k-(h-1)}} R(-2h\omega - \beta_j) & \sum_{j=1}^{m_{k-(h-1)}} R(-\alpha_j) \end{pmatrix} \begin{pmatrix} \mu \\ \nu \end{pmatrix}.$$

Proof (by induction on k): Fix an arbitrary $h \geq 1$ for the remainder of this proof.
$k = h$:

$$\Psi^h_h \begin{pmatrix} \mu \\ \nu \end{pmatrix} = \Omega^{-h}\Phi\Omega^h \begin{pmatrix} \mu \\ \nu \end{pmatrix}$$

$$= \frac{1}{5} \begin{pmatrix} R(0) + R(\pi) & 2R(2h\omega + \pi) + R(2h\omega - \frac{\pi}{2}) \\ 2R(-2h\omega - \pi) + R(-2h\omega + \frac{\pi}{2}) & R(-0) + R(-\pi) \end{pmatrix} \begin{pmatrix} \mu \\ \nu \end{pmatrix}.$$

Induction step: $\Psi^{k+1}_h \begin{pmatrix} \mu \\ \nu \end{pmatrix} = \Psi^{k+1}_{k+1}\Psi^k_h \begin{pmatrix} \mu \\ \nu \end{pmatrix}$. We know what Ψ^{k+1}_{k+1} looks like from our base case above, and we have Ψ^k_h by the induction hypothesis. To continue this

argument in matrix form becomes too wide for a single page, and hence we will start considering Ψ_h^{k+1} componentwise and cease carrying the pair of measures along. Also, we note that $\frac{1}{5}\cdot\frac{1}{5^{k-(h-1)}} = \frac{1}{5^{(k+1)-(h-1)}}$ and we will therefore suppress matrix coefficients for the time being. Because of the symmetry of the Ψ matrices, we need only consider $(\Psi_h^{k+1})_{11}$ and $(\Psi_h^{k+1})_{12}$:

$$\begin{aligned}(\Psi_h^{k+1})_{11} &= (R(0)+R(\pi))\sum_{j=1}^{m_{k-(h-1)}} R(\alpha_j) \\ &\quad + (2R(2(k+1)\omega+\pi)+R(2(k+1)\omega-\frac{\pi}{2})\sum_{j=1}^{n_{k-(h-1)}} R(-2h\omega-\beta_j) \\ &= \sum_{j=1}^{m_{k-(h-1)}} R(\alpha_j)+\sum_{j=1}^{m_{k-(h-1)}} R(\alpha_j+\pi)+\sum_{j=1}^{n_{k-(h-1)}} 2R(2(k-(h-1))\omega-\beta_j+\pi) \\ &\quad + \sum_{j=1}^{n_{k-(h-1)}} R(2(k-(h-1))\omega-\beta_j-\frac{\pi}{2}).\end{aligned}$$

We need to show $(\Psi_h^{k+1})_{11} = \sum_{j=1}^{m_{(k+1)-(h-1)}} R(\alpha_j)$. We know that $\{\alpha_j\}_{j=1}^{m_{(k+1)-(h-1)}}$ is the list of the angles of the orientations of the control points of positive chirality in $\Lambda_{(k+1)-(h-1)}$, and hence is composed of two rotated copies of $\{\alpha_j\}_{j=1}^{m_{k-(h-1)}}$ as well as three reflected and rotated copies of $\{\beta_j\}_{j=1}^{m_{k-(h-1)}}$. We know that the α_j terms of $(\Psi_h^{k+1})_{11}$ are correct. Now, $\{-\beta_j\}_{j=1}^{m_{k-(h-1)}}$ is the list of all angles of orientations of control points of positive chirality in $V_{k-(h-1)}$, the reflection of $\Lambda_{k-(h-1)}$ in the real axis (see Definition 2.13) . We need only to rotate this list into the proper orientations. Since $\Lambda_{k-(h-1)}$ has orientation $(k-(h-1))\omega$ and $V_{k-(h-1)}$ has orientation $-(k-(h-1))\omega$, rotating $V_{k-(h-1)}$ through $2(k-(h-1))\omega$ gives it the same orientation as $\Lambda_{k-(h-1)}$. A final rotation through π or $-\frac{\pi}{2}$ drops the copy $\{-\beta_j\}_{j=1}^{m_{k-(h-1)}}$ into the correct orientation to help make up $\{\alpha_j\}_{j=1}^{m_{(k+1)-(h-1)}}$ (For help visualizing this argument, see Figure 13). Hence, $(\Psi_h^{k+1})_{11} = \sum_{j=1}^{m_{(k+1)-(h-1)}} R(\alpha_j)$.

By a very similar argument, we get

$$\begin{aligned}
(\Psi_h^{k+1})_{12} &= (R(0)+R(\pi)) \sum_{j=1}^{n_{k-(h-1)}} R(2h\omega+\beta_j) \\
&\quad + (2R(2(k+1)\omega+\pi) + R(2(k+1)\omega-\frac{\pi}{2}) \sum_{j=1}^{m_{k-(h-1)}} R(-\alpha_j) \\
&= \sum_{j=1}^{n_{k-(h-1)}} R(2h\omega+\beta_j) + \sum_{j=1}^{n_{k-(h-1)}} R(2h\omega+\beta_j+\pi) \\
&\quad + \sum_{j=1}^{m_{k-(h-1)}} 2R(2(k+1)\omega-\alpha_j+\pi) + \sum_{j=1}^{m_{k-(h-1)}} R(2(k+1)\omega-\alpha_j-\frac{\pi}{2}) \\
&= R(2h\omega)\Big(\sum_{j=1}^{n_{k-(h-1)}} R(\beta_j) + \sum_{j=1}^{m_{k-(h-1)}} 2R(2(k-(h-1))\omega-\alpha_j+\pi) \\
&\quad + \sum_{j=1}^{n_{k-(h-1)}} R(\beta_j+\pi) + \sum_{j=1}^{m_{k-(h-1)}} R(2(k-(h-1))\omega-\alpha_j-\frac{\pi}{2})\Big) \\
&= R(2h\omega)\Big(\sum_{j=1}^{n_{(k+1)-(h-1)}} R(\beta_j)\Big) \\
&= \sum_{j=1}^{n_{(k+1)-(h-1)}} R(2h\omega+\beta_j)\,.
\end{aligned}$$

□

From the above argument, we can see that $(M(t))^k$ and Ψ_1^k are somewhat related, but handle reflections in very different ways! Now that we understand Ψ_h^k in terms of our sequences of angles, we can put the uniform distribution result to good use.

Proposition 4.16 *For any $u \in \mathcal{P}$ and uniformly distributed sequence $\{z_n\}_{n=1}^{\infty} \subset U(1)$ we have:*

$$\lim_{N\to\infty} \frac{1}{N} \sum_{n=1}^{N} R(z_n)\delta_u = \lambda^{U(1)} \otimes \delta_{|u|}\,,$$

where the limit is in the vague topology.

Proof. Note that the product of measures above refers to the product decomposition $\mathcal{P} = U(1) \times \mathbb{R}_{>0}$.

Let f be any continuous compactly supported $\mathbb{C}$-valued function on $\mathcal{P}$. We are required to show that

$$\lim_{N\to\infty}\left\langle \frac{1}{N}\sum_{n=1}^{N} R(z_n)\delta_u, f\right\rangle = \langle \lambda^{U(1)}\otimes\delta_{|u|}, f\rangle\,.$$

We have

$$\begin{aligned}
\left\langle \frac{1}{N}\sum_{n=1}^{N} R(z_n)\delta_u, f\right\rangle &= \frac{1}{N}\sum_{n=1}^{N}\langle \delta_u, R(z_n)^{-1}f\rangle \\
&= \frac{1}{N}\sum_{n=1}^{N}\int_{\mathcal{P}} f(z_n x)\,d\delta_u(x) = \frac{1}{N}\sum_{n=1}^{N} f(z_n u) \\
&\overset{N\to\infty}{\longrightarrow} \int_{U(1)} f(zu)dz = \int_{U(1)} f(z\,|u|)dz \\
&= \int_{U(1)\times\mathbb{R}_{>0}} f(zr)\,d\lambda^{U(1)}(z)\otimes\delta_{|u|}(r) = \langle \lambda^{U(1)}\otimes\delta_{|u|}, f\rangle
\end{aligned}$$

where, when calculating the limit, we have applied Definition 3.4 to the continuous function $f((.)u)$. □

It is important here to note that measures of the form $\lambda^{U(1)}\otimes\mu_K$, where μ_K is a positive measure on $K\subset(0,\infty)$, are not what one may intuitively think from the perspective of usual Lebesgue measure on $\mathbb{R}^2$. For example, consider that $\|\lambda^{U(1)}\otimes\mu_K\| = \lambda^{U(1)}(U(1))\mu_K(K) = \mu_K(K)$. This is independent of where K lies in $(0,\infty)$. Since the Lebesgue measure of B_K (see Definition 4.20) should be its area, it must depend on where K is located. Hopefully this comment will avert some confusion.

Proposition 4.16 can be extended by linearity to finitely supported discrete measures on $\mathcal{P}$, but we require some new notation before implementing this result.

Definition 4.17 *Let $P:\mathcal{P}\to(0,\infty)$ be defined by $P(z):=|z|$. Then P determines a linear map (also denoted by P) from $\mathcal{M}^*_{pp}(\mathcal{P})$ to $\mathcal{M}^\infty((0,\infty))$ by*

$$P(\sum_{k=1}^{n} c_k\delta_{a_k}) := \sum_{k=1}^{n} c_k\delta_{P(a_k)}\,.$$

Let $\mu,\nu\in\mathcal{M}^*_{pp}(\mathcal{P})$ be finitely supported discrete measures. Then we have:

Corollary 4.18 $\Psi_h^k\begin{pmatrix}\mu\\ \nu\end{pmatrix}\overset{k\to\infty}{\longrightarrow}\frac{1}{2}\begin{pmatrix}\lambda^{U(1)}\otimes(P(\mu+\nu))\\ \lambda^{U(1)}\otimes(P(\mu+\nu))\end{pmatrix}$ *in the vague topology.*

Proof: The combination of Propositions 4.15 and 4.16 yields

$$\begin{aligned}\Psi_h^k \begin{pmatrix} \delta_x \\ \delta_y \end{pmatrix} &\xrightarrow{k\to\infty} \frac{1}{2}\begin{pmatrix} \lambda^{U(1)} \otimes \delta_{|x|} + \lambda^{U(1)} \otimes \delta_{|y|} \\ \lambda^{U(1)} \otimes \delta_{|x|} + \lambda^{U(1)} \otimes \delta_{|y|} \end{pmatrix} \\ &= \frac{1}{2}\begin{pmatrix} \lambda^{U(1)} \otimes (\delta_{|x|} + \delta_{|y|}) \\ \lambda^{U(1)} \otimes (\delta_{|x|} + \delta_{|y|}) \end{pmatrix}\end{aligned}$$

for any $h \geq 1$.

As per the note following Proposition 4.16, the desired result follows by linearity. □

4.4 The Autocorrelation on the nth Iterate

We recall that Λ_n consists of 5 isometrical copies of Λ_{n-1}. This leads to the following definition:

Definition 4.19 *Let $n \geq 1$. Then*

$$\begin{aligned} D_n &:= \left\{(x,y) \in \Lambda \times \Lambda \;\middle|\; x,y \in \Lambda_n \text{ and are in different copies of } \Lambda_{n-1}\right\}, \\ C_n &:= \left\{(x,y) \in \Lambda \times \Lambda \;\middle|\; x,y \in \Lambda_n, x \neq y, \text{ and are in the same copy of } \Lambda_{n-1}\right\}. \end{aligned}$$

Remarks:

(i)

$$\eta_n = \delta_0 + \frac{1}{5^n}\sum_{x,y\in C_n} \delta_{x-y} + \frac{1}{5^n}\sum_{x,y\in D_n} \delta_{x-y}\,. \tag{4.1}$$

(ii) From the abutment atlas seen in Figure 6, we can see that the minimum distance between control points in the pinwheel tiling is $\frac{2}{\sqrt{5}}$ and results when their corresponding tiles abut hypotenuses and are of opposite chiralities. Then, there exists $\frac{2}{\sqrt{5}} > r > 0$ such that $\eta_n|_{B_r(0)} = \delta_0$. For such an r, $\lim_{n\to\infty} \eta_n|_{B_r(0)} = \delta_0$.

Definition 4.20 *For any K bounded in $(0,\infty)$, we define*

$$B_K := \left\{a \in \mathcal{P} \;\middle|\; |a| \in K\right\} = P^{-1}(K),$$

the **corona** *around 0 whose intersection with the positive x axis is K.*

Remark: For any $\mu, \nu \in \mathcal{M}^*_{pp}(\mathcal{P})$, we have:

(i) $\mu(B_K) = P(\mu)(K)$,

(ii) $\Psi_h^k \begin{pmatrix} \mu \\ \nu \end{pmatrix}(B_K) = \frac{1}{5^{k-(h-1)}} \begin{pmatrix} m_{k-(h-1)}\mu(B_K) + n_{k-(h-1)}\nu(B_K) \\ n_{k-(h-1)}\mu(B_K) + m_{k-(h-1)}\nu(B_K) \end{pmatrix}$.

Lemma 4.21 *For all $\nu, \nu' \geq 0$, we have*

$$\Psi_h^k \begin{pmatrix} \nu \\ \nu' \end{pmatrix}(B_K) \leq \begin{pmatrix} \nu(B_K) + \nu'(B_K) \\ \nu(B_K) + \nu'(B_K) \end{pmatrix}.$$

Proof (by induction on k):
$k = 0$: We have defined Ψ_1^0 to be the identity map previously.
Induction step: Let $\Psi_h^k \begin{pmatrix} \nu \\ \nu' \end{pmatrix} = \begin{pmatrix} \nu'' \\ \nu''' \end{pmatrix}$.
Then

$$\begin{aligned}
\Psi_h^{k+1} \begin{pmatrix} \nu \\ \nu' \end{pmatrix}(B_K) &= \Psi_{k+1}^{k+1}\Psi_h^k \begin{pmatrix} \nu \\ \nu' \end{pmatrix}(B_K) \\
&= \frac{1}{5} \begin{pmatrix} 2\nu''(B_K) + 3\nu'''(B_K) \\ 3\nu''(B_K) + 2\nu'''(B_K) \end{pmatrix} \\
&\leq \frac{1}{5} \begin{pmatrix} 2(\nu(B_K) + \nu'(B_K)) + 3(\nu(B_K) + \nu'(B_K)) \\ 3(\nu(B_K) + \nu'(B_K)) + 2(\nu(B_K) + \nu'(B_K)) \end{pmatrix} \\
&= \begin{pmatrix} \nu + \nu' \\ \nu + \nu' \end{pmatrix}(B_K)
\end{aligned}$$

by Definition 4.14, Remark (ii) above, the induction hypothesis, and simplification, respectively. □

We have successfully created our substitution formalism for measures. Since we wish to use it to compute the autocorrelation, we are going to need to feed it some measures.

Definition 4.22

(i) $\rho_n := \frac{1}{5^n} \sum_{x,y \in D_n} \delta_{x-y}$.

(ii) η_n^+, η_n^- *are defined recursively as follows:*
$\eta_1^+ = \eta_1^- := 0$,
$\begin{pmatrix} \eta_n^+ \\ \eta_n^- \end{pmatrix} := \Psi_{n-1}^{n-1} \begin{pmatrix} \eta_{n-1}^+ + \rho_{n-1} \\ \eta_{n-1}^- \end{pmatrix}$.

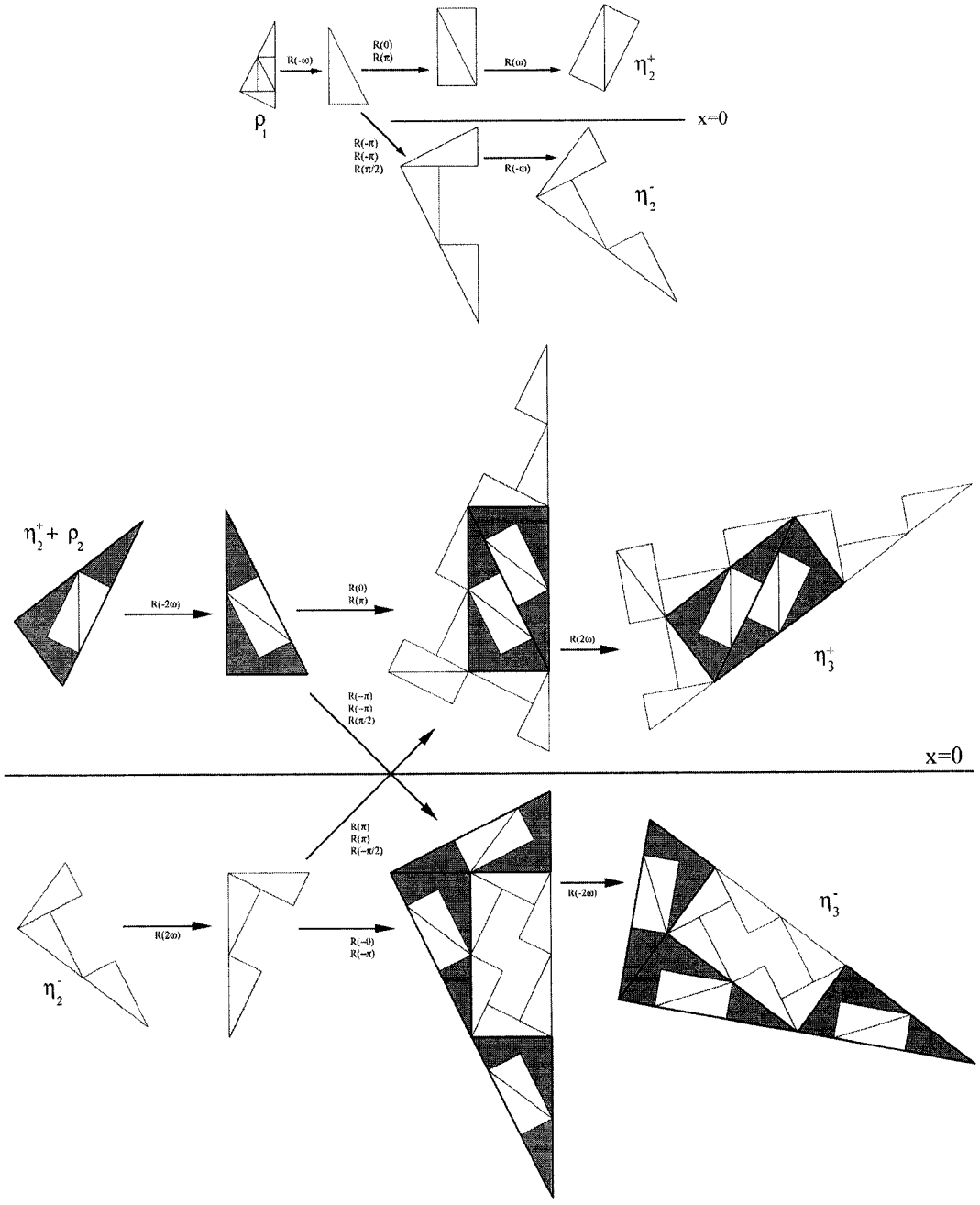

Figure 13: Ψ_1^1 and Ψ_2^2 in action

Lemma 4.23 $\begin{pmatrix} \eta_n^+ \\ \eta_n^- \end{pmatrix} = \sum_{k=1}^{n-1} \Psi_{n-k}^{n-1} \begin{pmatrix} \rho_{n-k} \\ 0 \end{pmatrix} \quad \forall\, n \geq 2\,.$

Proof (by induction on n):

$n = 2$: $\begin{pmatrix} \eta_2^+ \\ \eta_2^- \end{pmatrix} = \Psi_1^1 \begin{pmatrix} \eta_1^+ + \rho_1 \\ \eta_1^- \end{pmatrix} = \Psi_1^1 \begin{pmatrix} \rho_1 \\ 0 \end{pmatrix} = \sum_{k=1}^{1} \Psi_{2-k}^1 \begin{pmatrix} \rho_{2-k} \\ 0 \end{pmatrix}.$

Induction step: $\begin{pmatrix} \eta_{n+1}^+ \\ \eta_{n+1}^- \end{pmatrix} = \Psi_n^n \begin{pmatrix} \eta_n^+ + \rho_n \\ \eta_n^- \end{pmatrix} = \Psi_n^n \begin{pmatrix} \rho_n \\ 0 \end{pmatrix} + \Psi_n^n \begin{pmatrix} \eta_n^+ \\ \eta_n^- \end{pmatrix}$

$= \Psi_n^n \begin{pmatrix} \rho_n \\ 0 \end{pmatrix} + \Psi_n^n \left(\sum_{k=1}^{n-1} \Psi_{n-k}^{n-1} \begin{pmatrix} \rho_{n-k} \\ 0 \end{pmatrix} \right) = \Psi_n^n \begin{pmatrix} \rho_n \\ 0 \end{pmatrix} + \sum_{k=1}^{n-1} \Psi_{n-k}^n \begin{pmatrix} \rho_{n-k} \\ 0 \end{pmatrix}$

$= \sum_{k=1}^{(n+1)-1} \Psi_{n-k}^{(n+1)-1} \begin{pmatrix} \rho_{(n+1)-k} \\ 0 \end{pmatrix}.$ □

Proposition 4.24 *For any $n \geq 1$ we have*

$$\eta_n = \delta_0 + \eta_n^+ + \overline{\eta_n^-} + \rho_n\,. \tag{4.2}$$

Proof: To see that equation (4.2) holds, by (4.1) we must prove that

$$\eta_{n+1}^+ + \overline{\eta_{n+1}^-} = \frac{1}{5^{n+1}} \sum_{(x,y) \in C_{n+1}} \delta_{x-y}\,.$$

We prove this by induction. Figure 13 may help clarify the following argument (note that the gray represents ρ_2 rather than the tiles of negative chirality).

$n = 0$: $C_1 = \emptyset$; $\eta_1^+ = 0, \eta_1^- = 0$, which gives us our desired equality.

Induction step: Λ_{n+1} consists of the union of the five disjoint copies of Λ_n resulting from the application of the mappings $f_1, \ldots, f_5$ upon Λ_n. Here f_1, f_2 are direct isometries of $\mathbb{C}$, while f_3, f_4, f_5 are opposite (i.e., chirality reversing) isometries of $\mathbb{C}$ (note that the translation and reflection components of these isometries depend on n, while the rotation components are independent of n).

Then

$$\begin{aligned} C_{n+1} \;=\; & \big\{(x,y) \in \Lambda \times \Lambda \;\big|\; \exists\, 1 \leq i \leq 5 \text{ and } (a,b) \in \Lambda_n \times \Lambda_n \text{ with } a \neq b \\ & \text{such that } (x,y) = (f_i(a), f_i(b))\big\} \end{aligned}$$

$$\therefore \frac{1}{5^{n+1}} \sum_{(x,y)\in C_{n+1}} \delta_{x-y} = \frac{1}{5}\sum_{i=1}^{5} \frac{1}{5^n} \sum_{\substack{x,y\in\Lambda_n \\ x\neq y}} \delta_{f_i(x)-f_i(y)} \,.$$

The translation part of f_i cancels when we take differences:

$$\begin{aligned}\frac{1}{5^{n+1}} \sum_{(x,y)\in C_{n+1}} \delta_{x-y} &= \frac{1}{5}((R(0)+R(\pi))(\frac{1}{5^n}\sum_{\substack{x,y\in\Lambda_n \\ x\neq y}} \delta_{x-y}) \\ &\quad + \frac{1}{5}R(n\omega)(2R(\pi)+R(-\frac{\pi}{2}))\overline{R(-n\omega)(\frac{1}{5^n}\sum_{\substack{x,y\in\Lambda_n \\ x\neq y}} \delta_{x-y})}\,.\end{aligned}$$

Now, by the induction hypothesis:

$$\frac{1}{5^n}\sum_{\substack{x,y\in\Lambda_n \\ x\neq y}} \delta_{x-y} = \eta_n - \delta_0 \overset{(3.1)}{=} \eta_n^+ + \rho_n + \overline{\eta_n^-}\,.$$

Therefore,

$$\begin{aligned}\frac{1}{5^{n+1}} \sum_{(x,y)\in C_{n+1}} \delta_{x-y} &= \frac{1}{5}((R(0)+R(\pi))(\eta_n^+ + \rho_n + \overline{\eta_n^-}) \\ &\quad + \frac{1}{5}R(n\omega)(2R(\pi)+R(-\frac{\pi}{2}))\overline{R(-n\omega)(\eta_n^+ + \rho_n + \overline{\eta_n^-})} \\ &= \frac{1}{5}((R(0)+R(\pi))(\eta_n^+ + \rho_n + \overline{\eta_n^-}) \\ &\quad + \frac{1}{5}(2R(2n\omega+\pi)+R(2n\omega-\frac{\pi}{2}))(\overline{\eta_n^+} + \overline{\rho_n} + \eta_n^-) \\ &= \frac{1}{5}\Big((R(0)+R(\pi))(\eta_n^+ + \rho_n) + \overline{(R(-0)+R(-\pi))\eta_n^-} \\ &\quad + \overline{(2R(-2n\omega-\pi)+R(-2n\omega+\frac{\pi}{2}))(\eta_n^+ + \rho_n)} \\ &\quad + (2R(2n\omega+\pi)+R(2n\omega-\frac{\pi}{2}))\eta_n^-\Big) \\ &= \eta_{n+1}^+ + \overline{\eta_{n+1}^-}\end{aligned}$$

by Definition 4.22. □

4.5 Convergence and Circular Symmetry

Definition 4.25 $\mu_{n,K} := P(\eta_n|_{B_K}) \in \mathcal{M}^\infty((0,\infty))$ *for some* $K \subset (0,\infty)$ *bounded.*

Proposition 4.26 *Let $K \subseteq (0,\infty)$ be any bounded set. Then $\{\mu_{n,K}\}_{n=1}^{\infty}$ converges in the total variation norm topology to a pure point measure.*

Proof: By Definition 4.25 and Proposition 4.24, we get

$$\mu_{n+1,K} = P(\eta_{n+1}|_{B_K}) = P(\eta_{n+1}^+|_{B_K}) + P(\eta_{n+1}^-|_{B_K}) + P(\rho_{n+1}|_{B_K}).$$

Note that $P(\eta_{n+1}^-) = P(\overline{\eta_{n+1}^-})$.

By a remark following Definition 4.20, if $K' \subseteq K$ is any set we have

$$\begin{pmatrix} \eta_{n+1}^+(B_{K'}) \\ \eta_{n+1}^-(B_{K'}) \end{pmatrix} = \frac{1}{5}\begin{pmatrix} 2\eta_n^+(B_{K'}) + 2\rho_n(B_{K'}) + 3\eta_n^-(B_{K'}) \\ 3\eta_n^+(B_{K'}) + 3\rho_n(B_{K'}) + 2\eta_n^-(B_{K'}) \end{pmatrix},$$

whence

$$\begin{aligned} P(\eta_{n+1}^+)(K') + P(\eta_{n+1}^-)(K') &= \eta_{n+1}^+(B_{K'}) + \eta_{n+1}^-(B_{K'}) \\ &= \eta_n^+(B_{K'}) + \eta_n^-(B_{K'}) + \rho_n(B_{K'}) \\ &= \eta_n(B_{K'}) \\ &= P(\eta_n)(K'). \end{aligned}$$

Thus, for all $K' \subseteq K$ we have $P(\eta_{n+1}^+)(K') + P(\eta_{n+1}^-)(K') = P(\eta_n)(K')$.

Hence,

$$\begin{aligned} P(\eta_{n+1}^+|_{B_K}) + P(\eta_{n+1}^-|_{B_K}) &= P(\eta_{n+1}^+)|_K + P(\eta_{n+1}^-)|_K \\ &= P(\eta_n)|_K \\ &= P(\eta_n|_{B_K}) \\ &= \mu_{n,K}. \end{aligned}$$

So we get

$$\mu_{n+1,K} = \mu_{n,K} + P(\rho_{n+1}|_{B_K}). \tag{4.3}$$

Therefore, $\mu_{n+1,K} \geq \mu_{n,K}$ and

$$\|\mu_{n+1,K} - \mu_{n,K}\| = |P(\rho_{n+1}|_{B_K})| = \rho_{n+1}(B_K) = \frac{1}{5^{n+1}}\mathrm{card}\{(x,y) \in D_{n+1} \mid |x-y| \in K\}.$$

Because x, y must be in different copies of Λ_n, x must be in the B_K-boundary of one of those copies and $y \in x + B_K$. Let $c := \max_{a\in\mathbb{C}}(\mathrm{card}\{\Lambda \cap (a + B_K)\})$, a finite quantity because the minimum distance between control points is $\frac{2}{\sqrt{5}}$. Then,

$$\mathrm{card}\{(x,y) \in D_{n+1} \mid |x-y| \in K\} \leq c \cdot \sum_{j=1}^{5} \mathrm{card}\{x \in \Lambda \cap \partial^{B_K}(f_j\Gamma_n)\}.$$

When we inflate Γ_n we have $\lambda^{\mathbb{R}^2}(\partial^{B_K}\Gamma_{n+1}) \simeq \sqrt{5}\lambda^{\mathbb{R}^2}(\partial^{B_K}\Gamma_n)$, where $\lambda^{\mathbb{R}^2}$ is Lebesgue measure on $\mathbb{R}^2$, since the linear scaling is by $\sqrt{5}$.

Therefore, $\exists$ a constant c' depending only on K such that

$$\rho_{n+1}(B_K) \leq c' \left(\frac{1}{\sqrt{5}}\right)^{n+1}. \tag{4.4}$$

Then $\|\mu_{m,K} - \mu_{n,K}\| \leq c' \sum_{j=n+1}^{m} (\frac{1}{\sqrt{5}})^j$ shows that $\{\mu_{n,K}\}_n$ is Cauchy in the total variation norm. By a comment following Proposition 3 of [1], $\{\mu_{n,K}\}_n$ converges in the total variation norm topology to a pure point measure. □

Definition 4.27 $\mu_K := \lim_{n\to\infty} \mu_{n,K}$ *is a pure point measure on* $(0,\infty)$.

Proposition 4.28 $\eta_n|_{B_K} \longrightarrow \lambda^{U(1)} \otimes \mu_K$ *in the vague topology.*

Proof: Let $\eta_K = \lambda^{U(1)} \otimes \mu_K$. Let U be any neighbourhood of 0 in the vague topology. Then $\exists\, V$, a neighbourhood of 0, such that $V + V + V + V + V + V \subseteq U$. Also, we may assume that $V = -V$. Since the total variation topology is stronger than the vague topology, $\exists\, \epsilon > 0$ such that whenever $\|\nu\| < \epsilon$, $\nu \in V$.

Because $\mu_{n,K} \xrightarrow{\|\cdot\|} \mu_K$, there exists N such that for all $n > N$, we have $\|\mu_{n,K} - \mu_K\| < \epsilon$. This gives us $\|\lambda^{U(1)} \otimes \mu_{n,K} - \lambda^{U(1)} \otimes \mu_K\| < \epsilon$, and hence, $\lambda^{U(1)} \otimes \mu_{n,K} - \eta_K \in V \;\forall\, n > N$.

(4.4) says that $\rho_n(B_K) \leq c' \left(\frac{1}{\sqrt{5}}\right)^n$, so $\exists\, M \geq N+1$ such that

$$\sum_{k=M}^{m} \rho_k(B_K) < \epsilon \;\; \forall\, m \geq M.$$

We know by Lemma 4.23 that

$$\begin{pmatrix} \eta_n^+|_{B_K} \\ \eta_n^-|_{B_K} \end{pmatrix} = \sum_{k=1}^{n-1} \Psi_{n-k}^{n-1} \begin{pmatrix} \rho_{n-k}|_{B_K} \\ 0 \end{pmatrix}. \tag{4.5}$$

Splitting the above sum yields

$$\begin{pmatrix} \eta_{n+M}^+|_{B_K} \\ \eta_{n+M}^-|_{B_K} \end{pmatrix} - \Psi_M^{n+M-1} \begin{pmatrix} \eta_M^+|_{B_K} \\ \eta_M^-|_{B_K} \end{pmatrix} = \sum_{k=1}^{n} \Psi_{n+M-k}^{n+M-1} \begin{pmatrix} \rho_{n+M-k}|_{B_K} \\ 0 \end{pmatrix},$$

and using the triangle inequality gets us

$$\left\| \begin{pmatrix} \eta_{n+M}^+|_{B_K} \\ \eta_{n+M}^-|_{B_K} \end{pmatrix} - \Psi_M^{n+M-1} \begin{pmatrix} \eta_M^+|_{B_K} \\ \eta_M^-|_{B_K} \end{pmatrix} \right\| \leq \sum_{k=1}^{n} \left| \Psi_{n+M-k}^{n+M-1} \begin{pmatrix} \rho_{n+M-k} \\ 0 \end{pmatrix} \right| (B_K)$$

$$= \sum_{k=1}^{n} \Psi_{n+M-k}^{n+M-1} \begin{pmatrix} \rho_{n+M-k} \\ 0 \end{pmatrix} (B_K),$$

where $\left\| \begin{pmatrix} \nu \\ \nu' \end{pmatrix} \right\| := \begin{pmatrix} \|\nu\| \\ \|\nu'\| \end{pmatrix}$ and $\|\cdot\|$ is the total variation norm.

Thus, by Lemma 4.21 and (4.5),

$$\left| \begin{pmatrix} \eta_{n+M}^{+} \\ \eta_{n+M}^{-} \end{pmatrix} - \Psi_{M}^{n+M-1} \begin{pmatrix} \eta_{M}^{+} \\ \eta_{M}^{-} \end{pmatrix} \right| (B_K) < \begin{pmatrix} \epsilon \\ \epsilon \end{pmatrix}. \tag{4.6}$$

We also know that $\lambda^{U(1)} \otimes \mu_{M-1} - \eta_K \in V$. From Corollary 4.18 and the fact that M is fixed, we know

$$\Psi_{M}^{n+M-1} \begin{pmatrix} \eta_{M}^{+}|_{B_K} \\ \eta_{M}^{-}|_{B_K} \end{pmatrix} \xrightarrow{n\to\infty} \frac{1}{2} \begin{pmatrix} \lambda^{U(1)} \otimes P(\eta_{M}^{+}|_{B_K} + \eta_{M}^{-}|_{B_K}) \\ \lambda^{U(1)} \otimes P(\eta_{M}^{+}|_{B_K} + \eta_{M}^{-}|_{B_K}) \end{pmatrix}$$

and so, by (4.3), we get that

$$\Psi_{M}^{n+M-1} \begin{pmatrix} \eta_{M}^{+}|_{B_K} \\ \eta_{M}^{-}|_{B_K} \end{pmatrix} \xrightarrow{n\to\infty} \frac{1}{2} \begin{pmatrix} \lambda^{U(1)} \otimes \mu_{M-1} \\ \lambda^{U(1)} \otimes \mu_{M-1} \end{pmatrix}.$$

Therefore, $\exists\, N'$ such that

$$\Psi_{M}^{n+M-1} \begin{pmatrix} \eta_{M}^{+}|_{B_K} \\ \eta_{M}^{-}|_{B_K} \end{pmatrix} - \frac{1}{2} \begin{pmatrix} \lambda^{U(1)} \otimes \mu_{M-1} \\ \lambda^{U(1)} \otimes \mu_{M-1} \end{pmatrix} \in \begin{pmatrix} V \\ V \end{pmatrix} \quad \forall\, n \geq N',$$

and by (4.6), we have

$$\begin{pmatrix} \eta_{n+M}^{+}|_{B_K} \\ \eta_{n+M}^{-}|_{B_K} \end{pmatrix} - \Psi_{M}^{n+M-1} \begin{pmatrix} \eta_{M}^{+}|_{B_K} \\ \eta_{M}^{-}|_{B_K} \end{pmatrix} \in \begin{pmatrix} V \\ V \end{pmatrix} \quad \forall\, n \geq 0.$$

Combining the above, we get

$$\begin{pmatrix} \eta_{n+M}^{+}|_{B_K} \\ \eta_{n+M}^{-}|_{B_K} \end{pmatrix} - \frac{1}{2} \begin{pmatrix} \lambda^{U(1)} \otimes \mu_{M-1} \\ \lambda^{U(1)} \otimes \mu_{M-1} \end{pmatrix} \in \begin{pmatrix} V - V \\ V - V \end{pmatrix} \quad \forall\, n \geq N'.$$

So, by Proposition 4.24

$$\begin{aligned} \eta_{n+M}|_{B_K} - \eta_K \;=\; & (\eta_{n+M}^{+}|_{B_K} - \frac{1}{2}\lambda^{U(1)} \otimes \mu_{M-1}) + (\eta_{n+M}^{-}|_{B_K} - \frac{1}{2}\lambda^{U(1)} \otimes \mu_{M-1}) \\ & + (\lambda^{U(1)} \otimes \mu_{M-1} - \lambda^{U(1)} \otimes \mu_K) + \rho_{n+M}|_{B_K}. \end{aligned}$$

Also, (4.5) gives us

$$\|\rho_{n+M}|_{B_K}\| < \epsilon \implies \rho_{n+M}|_{B_K} \in V\,.$$

Thus

$$\eta_{n+M}|_{B_K} - \eta_K \in V - V + V - V + V + V \subseteq U\,,$$

and therefore $\eta_n|_{B_K} - \eta_K \in U \;\; \forall\, n > N' + M\,.$ □

4.6 Autocorrelation Conclusions

It is easy to see that if $K \subseteq K'$ then $\mu_{K'}|_K = \mu_K$. This allows the following definition:

Definition 4.29 *μ is the pure point measure on $(0,\infty)$ defined by $\mu|_K = \mu_K \;\forall\, K$ bounded in $(0,\infty)$.*

From Proposition 4.28 and the fact that $\lim_{n\to\infty} \eta_n|_{B_r(0)} = \delta_0$ for some sufficiently small $r > 0$, we get that $\eta_n|_{\{0\}\cup B_K} \longrightarrow \delta_0 + \lambda^{U(1)} \otimes \mu|_K \;\forall\, K \subseteq (0,\infty)$ bounded. This final remark sets us up for the ultimate theorem of this chapter.

Theorem 4.30 *The autocorrelation of Λ, η, exists with respect to $\{\Lambda_n\}_{n=1}^{\infty}$ and $\eta = \frac{1}{4}(\delta_0 + \lambda^{U(1)} \otimes \mu)$.*

Proof: Suppose that f is an arbitrary real valued continuous function of compact support. Then, $\mathrm{supp}(f) \subseteq \{0\} \cup B_K$ for some bounded $K \subset (0,\infty)$.

From Proposition 4.28 we have

$$\eta_n|_{\{0\}\cup B_K} \longrightarrow \delta_0 + \lambda^{U(1)} \otimes \mu_K\,,$$

which means

$$\eta_n|_{\{0\}\cup B_K}(f) \longrightarrow (\delta_0 + \lambda^{U(1)} \otimes \mu_K)(f).$$

Because $\mathrm{supp}(f) \subseteq \{0\} \cup B_K$, this gives us

$$\eta_n(f) \longrightarrow (\delta_0 + \lambda^{U(1)} \otimes \mu)(f)\,,$$

and finally, by the definition of vague convergence,

$$\eta_n \longrightarrow \delta_0 + \lambda^{U(1)} \otimes \mu\,.$$

□

In this section, we have defined the autocorrelation and have calculated it to be the product of normalized Haar measure on $U(1)$ and a pure point measure on $(0, \infty)$, plus δ_0. This measure has pure point part consisting of the one delta peak at the origin, many singular continuous circles, and no absolutely continuous part; the first 48 circles are illustrated in Figure 14. Our understanding of the autocorrelation of the pinwheel tiling only lacks knowledge about the pure point measure μ, and hence about the radii and heights of the circles. In [11], Charles Radin suggests that the support of μ has a self-similar structure. While we were not able to exploit this observation, it may prove useful to future pinwheel enthusiasts.

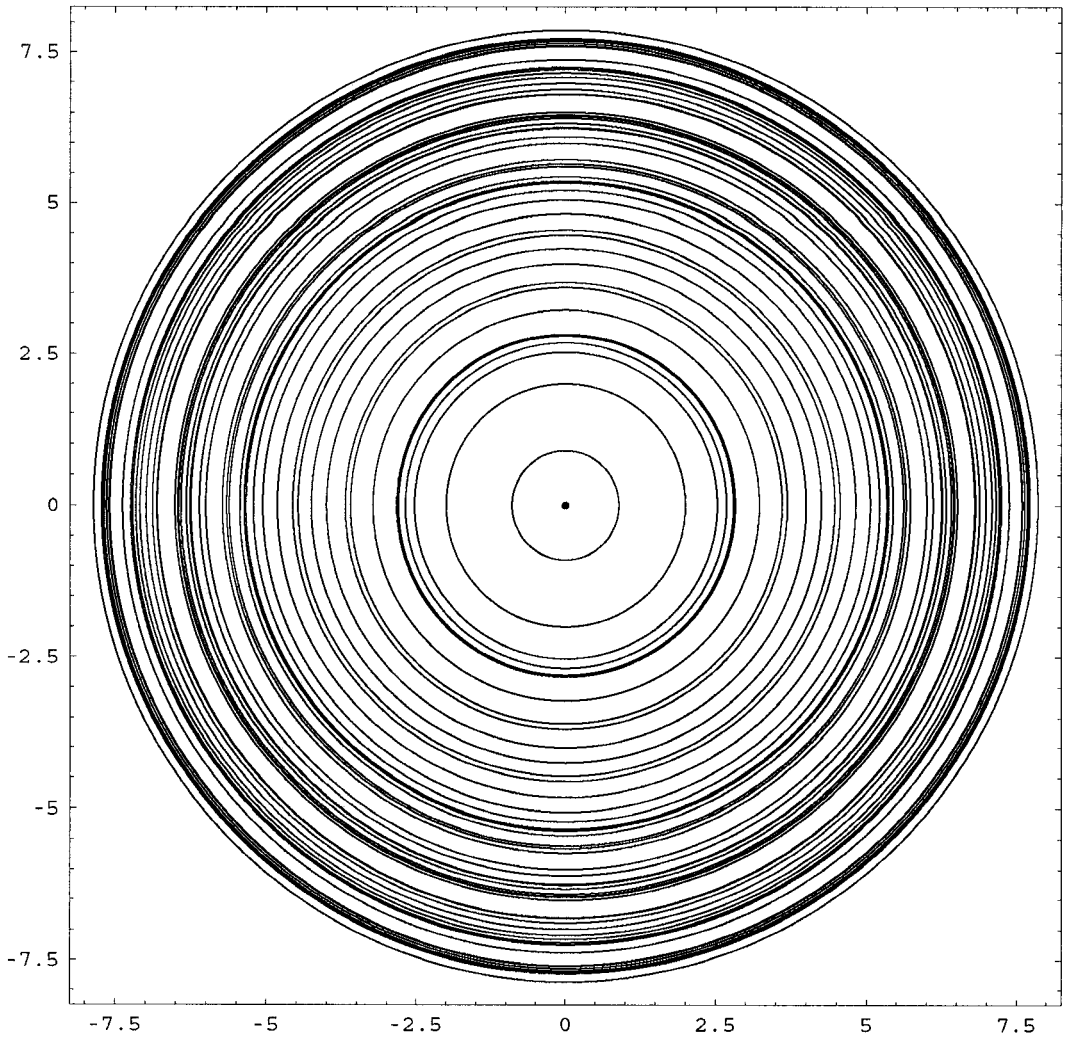

Figure 14: Part of the support of the pinwheel autocorrelation measure η

Chapter 5 - Diffraction and Outlook

We have worked hard to learn as much about the autocorrelation of the pinwheel tiling as possible, and have met with some success. To some extent, that work was a precursor to this section. Ultimately, we would like to compute the diffraction of the pinwheel tiling in order to learn more about its structure. The diffraction is helpful in this respect because it extracts information about the long range order from a tiling, information that is often shrouded in the tiling by local order. Unfortunately, calculating the diffraction of the pinwheel tiling in its full splendor is beyond the scope of this thesis. Even if we had a complete understanding of the autocorrelation – which we do not – the calculation of the diffraction is far from a straightforward process. In this chapter, we have two goals. First, we will provide the definition of the diffraction, and illuminate as much of its structure as we can. We will then finish with a summary of possible directions that pinwheel research could continue from here.

5.1 Diffraction

The diffraction of an object is the Fourier transform of its autocorrelation measure. To make any sense of this statement, we will require at least a cursory understanding of Fourier analysis on locally compact abelian groups. [3] is a thorough reference for this subject, and should be considered as the resource for all of the following material unless otherwise noted. Prior to starting with the definitions, we note that Proposition 7 of [2] tells us that η_n, η are all translation bounded, positive-definite, and positive measures; the positive-definiteness proves to be particularly important.

Definition 5.1 *For $f \in \mathcal{K}(\mathbb{R}^2)$, the* **Fourier transform** *of f is defined as*

$$\widehat{f}(k) := \int_{\mathbb{R}^2} e^{-2\pi i k \cdot x} f(x) dx \; \forall \, k \in \mathbb{R}^2 .$$

In the general definition, k belongs to the dual group of the group that f is defined on. In our case, both groups are $\mathbb{R}^2$. This is convenient, but one should be careful to remember that there are actually two groups involved to avoid confusion.

Definition 5.2 *For a finite measure ν on $\mathbb{R}^2$, the* **Fourier transform** *of ν is defined by the function*

$$\widehat{\nu}(k) := \int_{\mathbb{R}^2} e^{-2\pi i k \cdot x} d\nu(x) \; \forall \, k \in \mathbb{R}^2 .$$

Proposition 5.3 *For $f \in \mathcal{K}(\mathbb{R}^2)$ and $n \geq 1$, $\langle \widehat{\eta_n}, f \rangle = \langle \eta_n, \widehat{f} \rangle$.*

Proof:

$$\begin{aligned}
\langle \eta_n, \widehat{f} \rangle &= \int_{\mathbb{R}^2} \widehat{f}(k) d\eta_n(k) \\
&= \int_{\mathbb{R}^2} \int_{\mathbb{R}^2} e^{-2\pi i k \cdot x} f(x) d\lambda^{\mathbb{R}^2}(x)\, d\eta_n(k) \\
&= \frac{1}{5^n} \sum_{y,z \in \Lambda_n} \int_{\mathbb{R}^2} e^{-2\pi i (y-z) \cdot x} f(x) d\lambda^{\mathbb{R}^2}(x) \\
&= \frac{1}{5^n} \int_{\mathbb{R}^2} f(x) \Big(\sum_{y,z \in \Lambda_n} e^{-2\pi i x \cdot (y-z)} \Big) d\lambda^{\mathbb{R}^2}(x) \\
&= \int_{\mathbb{R}^2} f(x) \widehat{\eta_n}(x) d\lambda^{\mathbb{R}^2}(x) \\
&= \int_{\mathbb{R}^2} f(x) d\widehat{\eta_n}(x) \\
&= \langle \widehat{\eta_n}, f \rangle .
\end{aligned}$$

□

From Theorem 4.16 in [3], we know that Fourier transformation is a homeomorphism on the set of all positive and positive-definite measures on $\mathbb{R}^2$ equipped with the vague topology. Hence, because we know $\{\eta_n\}_n \overset{n\to\infty}{\longrightarrow} \eta$ in the vague topology, we know that $\{\widehat{\eta_n}\}_n$ also converges vaguely as $n \to \infty$.

Definition 5.4 *The* **diffraction** *of the pinwheel tiling is the Fourier transform of its autocorrelation, $\widehat{\eta} := \frac{1}{4} \lim_{n\to\infty} \widehat{\eta_n}$ (where this is a vague limit).*

By Proposition 7 of [2], we know that $\widehat{\eta}$ is a positive, transform bounded measure on $\mathbb{R}^2$. With minimal effort, we can make a few more deductions regarding the nature of $\widehat{\eta}$.

Lemma 5.5 *For $R(\alpha) \in U(1)$, $f \in \mathcal{K}(\mathbb{R}^2)$ we have:*

$$(R(\alpha)\widehat{f})(k) = \widehat{R(\alpha) f}(k)\,.$$

Proof:

$$\begin{aligned}
(R(\alpha)\widehat{f})(k) &= \widehat{f}(R(-\alpha)k) \\
&= \int e^{-2\pi i R(-\alpha)k\cdot x} f(x)dx \\
&= \int e^{-2\pi i k\cdot R(\alpha)x} f(x)dx \quad \text{(by rotational invariance of dot product)} \\
&= \int e^{-2\pi i k\cdot y} f(R(-\alpha)y)dy \quad \text{(by rot. invariance of Lebesgue measure)} \\
&= \widehat{R(\alpha)f}(k)\,.
\end{aligned}$$

□

Proposition 5.6 *Let σ be a Fourier transformable measure. If $R(\alpha)\sigma = \sigma$ then $\widehat{\sigma}(R(\alpha)f) = \widehat{\sigma}(f)$.*

Proof: Suppose $R(\alpha)\sigma = \sigma$. Then

$$\begin{aligned}
\widehat{\sigma}(R(\alpha)f) &= \sigma(\widehat{R(\alpha)f}) \\
&= \sigma(R(\alpha)\widehat{f}) \\
&= (R(-\alpha)\sigma)(\widehat{f}) \\
&= \sigma(\widehat{f}) \\
&= \widehat{\sigma}(f)\,.
\end{aligned}$$

□

Proposition 5.6 shows that any rotational symmetry possessed by the autocorrelation will also appear in the diffraction. Since the pinwheel autocorrelation is fully circularly symmetric, so is the diffraction. From this, we can see that the diffraction may only have a pure point part at the origin. We show that this is indeed the case.

Proposition 5.7 $\widehat{\eta}_{pp} = (dens(\Lambda))^2\delta_0$.

Proof: This result follows from Theorem 2.2 in [9]. We have

$$\begin{aligned}
m_0 &= \lim_{n\to\infty} \frac{1}{\mathrm{vol}(\Gamma_n)} \int 1\, d(\sum_{x\in\Lambda_n} \delta_x) \\
&= \lim_{n\to\infty} \frac{\mathrm{card}(\Lambda_n)}{\mathrm{vol}(\Gamma_n)} \\
&= \mathrm{dens}(\Lambda)\,.
\end{aligned}$$

Then, by the result mentioned above, $\widehat{\eta}(\{0\}) = (dens(\Lambda))^2$. □

For finite point sets, such as our Λ_n, there is an equivalent definition of diffraction that is more amenable to calculations. This definition is the one most often used by physicists, who always work with finite structures. The two paths to diffraction are often represented by a figure known as the Wiener diagram.

Definition 5.8 *The diffraction of* Λ_n *is alternately defined as*

$$\frac{1}{4}\widehat{\eta_n}(k) := \frac{1}{4 \cdot 5^n}\Big|\sum_{x \in \Lambda_n} e^{-2\pi i k \cdot x}\Big|^2.$$

We can compute this in a straightforward fashion by inputting values for k (though our value choices could certainly produce artifacting, or miss peaks altogether if our mesh size is too great). As was noted at the end of Chapter 1, the exponential growth in the number of control points puts a severe limit on our choice of n. Since the number of orientations grows linearly with n, the diffraction images we obtain via such computations will not be very good approximations of $\widehat{\eta}$ at all. Nonetheless, bearing these remarks in mind, such images may provide some insight. The code used to generate Figures 15 and 16 may be found in the Appendix.

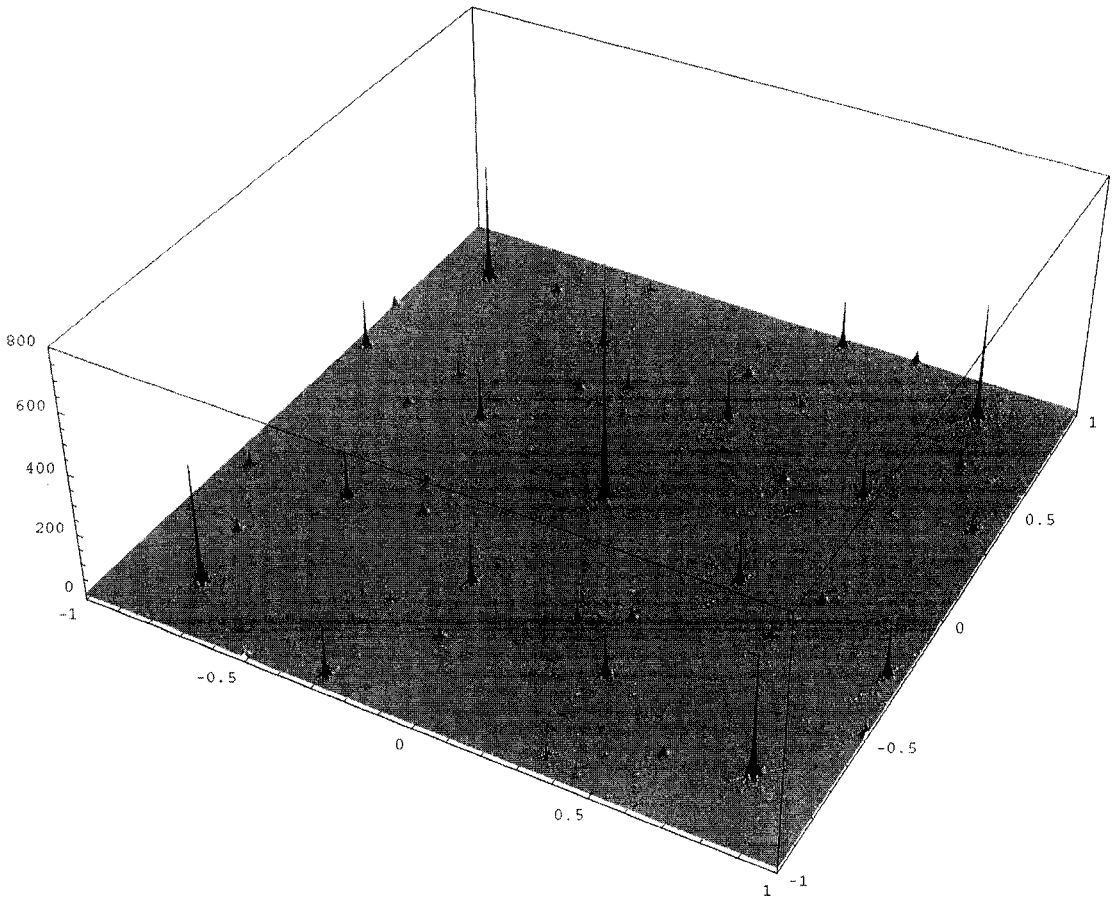

Figure 15: The diffraction of Λ_5

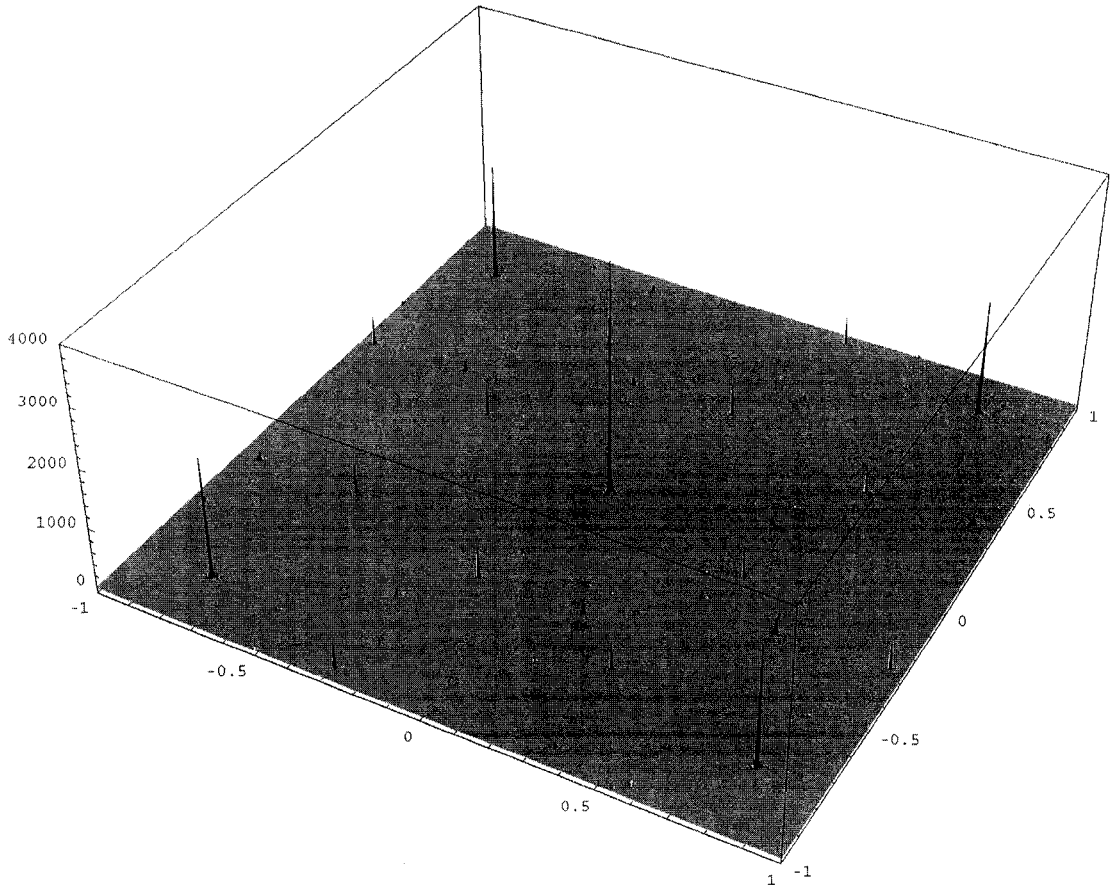

Figure 16: The diffraction of Λ_6

5.2 Outlook

As is perhaps most evident in the previous section on diffraction, there is yet much to learn about the pinwheel tiling. Recall that our analysis of the pinwheel autocorrelation $\eta = \frac{1}{4}(\delta_0 + \lambda^{U(1)} \otimes \mu)$ in Chapter 4 was incomplete. A continuing goal is to fully compute the pure point measure μ. Starting with a fully computed autocorrelation measure would increase the possibility of being able to obtain the diffraction measure of the pinwheel. In particular, another major goal is to compute the Lebesgue decomposition of the diffraction measure along a single ray emanating from the origin. By circular symmetry, we would then know the entire diffraction pattern.

The approach used in this thesis has been quite successful, but there are other possibilities. Many other aperiodic substitution tilings have been explained exceptionally fruitfully using a cut-and-project formalism. Unfortunately, we cannot use the same approach on the pinwheel tiling because it fails to exhibit finite local complexity due to its infinite tile orientations. If one considered patches of tiles to be equivalent up to translation and rotation, they might be able to obtain a finite local complexity result. We met the noncommutative group $E(2) = U(1) \ltimes \mathbb{R}^2$ in Chapter 2, and this is a much more natural setting for pinwheel considerations. In addition to the possibility of implementing a cut-and-project formalism, Chapter IV in [18] develops the Fourier transform on $E(2)$ and, based on this work, one should be able to calculate the noncommutative diffraction of the pinwheel tiling. This approach does have a few significant difficulties however. Because mathematical diffraction in $\mathbb{R}^2$ is directly related to physical diffraction phenomena, there is an extremely natural way to graphically interpret real diffraction patterns. There seems to be no such natural way to interpret noncommutative diffraction patterns, nor is any kind of physical analogue known. Moreover, in the real case, there is a vast canon of results available to aid in the diffraction analysis. While noncommutative analysis of the pinwheel would likely prove extremely fruitful, it is unfortunately well beyond the scope of a master's thesis. have been explained exceptionally fruitfully using a cut-and-project formalism. Unfortunately, we cannot use the same approach on the pinwheel tiling because it fails to exhibit finite local complexity due to its infinite tile orientations. If one considered patches of tiles to be equivalent up to translation and rotation, they might be able to obtain a finite local complexity result. We met the noncommutative group $E(2) = U(1) \ltimes \mathbb{R}^2$ in Chapter 2, and this is a much more natural setting for pinwheel considerations. In addition to the possibility of implementing a cut-and-project formalism, Chapter IV in [18] develops the Fourier transform on $E(2)$ and, based on this work, one should be able to calculate the noncommutative

diffraction of the pinwheel tiling. This approach does have a few significant difficulties however. Because mathematical diffraction in $\mathbb{R}^2$ is directly related to physical diffraction phenomena, there is an extremely natural way to graphically interpret real diffraction patterns. There seems to be no such natural way to interpret noncommutative diffraction patterns, nor is any kind of physical analogue known. Moreover, in the real case, there is a vast canon of results available to aid in the diffraction analysis. While noncommutative analysis of the pinwheel would likely prove extremely fruitful, it is unfortunately well beyond the scope of a master's thesis.

In [14], Sadun develops some generalizations of the pinwheel tiling. Whereas the canonical pinwheel tiling exhibits only one triangular tile up to reflection and rotation, Sadun creates pinwheel like tilings consisting of multiple similar right triangles. As he notes, this suggests an extension of the theory from the translation group to the conformal group, and not just to the Euclidean motion group as I have proposed above.

Sadun's generalized pinwheels are not the only other tilings exhibiting infinite tile orientations. In [10], Penrose presents a substitution tiling based on an isosceles triangle that manifests this property. It would be interesting to analyze this tiling and compare it to what we have learned of the pinwheel tiling. Specifically, it would be valuable to generalize the formalism we developed in Chapter 4 to other infinite orientation tilings such as Penrose's. It would also be valuable to compile a list of infinite orientation tilings, with the ultimate goal of classifying them.

Several tilings of space involving infinite orientations have been discovered, such as the quaquaversal tiling seen in [5]. Any developments in the two dimensional case would inevitably beg to be generalized to three or more dimensions.

Finally, it would be of incredible value if a physical substance with infinite orientation properties (like a glass) and long range order (like a crystal) were discovered or synthesized. Not only would such a substance lend resources and credibility to the examination of infinite orientation tilings, it might prove to have interesting physical characteristics. What we have learned of the pinwheel tiling suggests that it exhibits a type of order somewhere between that found in quasiperiodic tilings and that found in amorphous random tilings. Perhaps a physical analogue would likewise demonstrate a blend of the characteristics of quasicrystals and amorphous glasses.

Bibliography

[1] M. Baake and R.V. Moody, "Weighted Dirac Combs with Pure Point Diffraction", *Crelle J.* (in press) (2004), http://www.arxiv.org/math.MG/0203030

[2] M. Baake, R.V. Moody, and P.A.B. Pleasants, "Diffraction from Visible Lattice Points and kth Power Free Integers", *Disc. Math.* **221** (2000), 3-42.

[3] C. Berg and G. Forst, *Potential Theory on Locally Compact Abelian Groups*, Springer-Verlag, Berlin (1975).

[4] D.L. Cohn, *Measure Theory*, Birkhäuser, Boston (1980).

[5] J.H. Conway and C. Radin, "Quaquaversal Tilings and Rotations", *Invent. Math.* **132** (1998), 179-188.

[6] H.S.M. Coxeter, "Introduction to Geometry", Wiley, New York (1969).

[7] C. Goodman-Strauss, "Matching Rules and Substitution Tilings", *Annals of Math.* **147** (1998), 181-223.

[8] B. Grünbaum and G.C. Shephard, *Tilings and Patterns*, W.H. Freeman and Co, New York (1987).

[9] A. Hof, "Diffraction by Aperiodic Structures", in: *The Mathematics of Long-Range Aperiodic Order*, ed. R. V. Moody, NATO ASI Series C 489, Kluwer, Dordrecht (1997), 239-268.

[10] R. Penrose, "Remarks on Tiling: Details of a $(1 + \epsilon + \epsilon^2)$-Aperiodic Set", in: *The Mathematics of Long-Range Aperiodic Order*, ed. R. V. Moody, NATO ASI Series C 489, Kluwer, Dordrecht (1997), 467-498.

[11] C. Radin, "Symmetries of Quasicrystals" *J. Stat. Phys.* **95** (1999), 827-833.

[12] C. Radin, "Aperiodic Tilings, Ergodic Theory, and Rotations", in: *The Mathematics of Long-Range Aperiodic Order*, ed. R. V. Moody, NATO ASI Series C 489, Kluwer, Dordrecht (1997), 499-519.

[13] C. Radin, "The Pinwheel Tilings of the Plane", *Annals of Math.* **139** (1994), 661-702.

[14] L. Sadun, "Some Generalizations of the Pinwheel Tiling", *Disc. Comp. Geom.* **20** (1998), 79-110.

[15] M. Senechal, *Quasicrystals and Geometry*, Cambridge University Press, Cambridge (1995).

[16] E. Seneta, *Non-negative Matrices and Markov Chains*, Springer-Verlag, New York (1973).

[17] D. Shechtman, I. Blech, D. Gratias, and J.W. Cahn, "Metallic Phase with Long-Range Orientational Order and no Translational Symmetry", *Phys. Rev. Lett.* **53** (1984), 1951-1953.

[18] M. Sugiura, *Unitary Representations and Harmonic Analysis - An Introduction*, Kodansha, Tokyo (1975).

Appendix

The following is some of the Mathematica 5.0 code used to create the images seen throughout the thesis. There are certainly more efficient methods for performing the same calculations available to individuals with a more comprehensive understanding of computer programming.

The following code is derived from Proposition 3.2 and was used to create Figure 12. Different index ranges that are more Mathematica compatible are used below; notably, 1 denotes points of negative chirality and 2 denotes points of positive chirality for the fourth input argument. First, use the following to initialize the file oritable:

```
Zero[w_, x_, y_, z_] := (0)
init = Array[Zero, {2, 1, 4, 2}];
init[[1, 1, 1, 2]] = 1;
init[[2, 1, 1, 2]] = 1;
init[[2, 1, 3, 2]] = 1;
init[[2, 1, 3, 1]] = 2;
init[[2, 1, 4, 1]] = 1;
init >> oritable
```

The function OrientExpress returns a list of pairs consisting of an orientation and the number of times it occurs in the nth iterate:

```
Zero[w_, x_, y_, z_] := (0)
Opposite[chi_] := (
   If[chi == 1, 2, 1]
)
OneStep[n_] := (
   workingin = <<oritable;
   workingout = Array[Zero, {n, n - 1, 4, 2}];
   Do[workingout[[i, j, k, l]] = workingin[[i, j, k, l]], {i, 1, n - 1},
      {j, 1, n - 2}, {k, 1, 4}, {l, 1, 2}];
   Do[workingout[[n, j, k, l]] = (workingout[[n - 1, j, k, l]]
      + workingout[[n - 1, j, Mod[k - 1 + 2, 4] + 1, l]]
      + 2*workingout[[n - 1, n - j, Mod[2 - (k - 1), 4] + 1, Opposite[l]]]
      + workingout[[n - 1, n - j, Mod[3 - (k - 1), 4] + 1, Opposite[l]]]),
      {j, 1, n - 1}, {k, 1, 4}, {l, 1, 2}];
   workingout >> oritable
```

```
)
TableTake[n_, tab_] := (
    outlist = {};
    Do[outlist = Append[outlist, {{Mod[((a - 1)*Pi/2)
        - 2*(m - 1)*ArcTan[.5], 2*Pi], (-1)^e}, tab[[n, m, a, e]]}],
        {m, 1, n - 1}, {a, 1, 4}, {e, 1, 2}];
    outlist
)
TableMake[n_, tabsize_] := (
    Do[OneStep[i], {i, tabsize + 1, n}];
    new = << oritable;
    outlist = {};
    Do[outlist = Append[outlist, {{Mod[((a - 1)*Pi/2)
        - 2*(m - 1)*ArcTan[.5], 2*Pi], (-1)^e}, new[[n, m, a, e]]}],
        {m, 1, n - 1}, {a, 1, 4}, {e, 1, 2}];
    outlist
)
OrientExpress[n_] := (
    old = <<oritable;
    oldsize = Dimensions[old][[1]];
    If[oldsize ≥ n, TableTake[n, old], TableMake[n, oldsize]]
)
```

The following code follows the pinwheel substitution and generates the control points of the nth iterate. Proposition 2.10 can then be applied to convert the control points to tiles for the purpose of creating tiling images, as in TileSubstitutionPlot below:

```
startpoint := {{1, 0}, {0, 0}, 1};
rotloc := {{2, 1}, {-1, 2}};
oria := {{2/Sqrt[5], 1/Sqrt[5]}, {-1/Sqrt[5], 2/Sqrt[5]}};
orib := {{2/Sqrt[5], -1/Sqrt[5]}, {1/Sqrt[5], 2/Sqrt[5]}};
oric := {{1/Sqrt[5], -2/Sqrt[5]}, {2/Sqrt[5], 1/Sqrt[5]}};
orid := {{1/Sqrt[5], 2/Sqrt[5]}, {-2/Sqrt[5], 1/Sqrt[5]}};
ninety := {{0, -1}, {1, 0}};

translate[{a_, b_, 1}] := (
    v = {orib.a, b, 1};
```

```
    w = {-orib.a, -2orid.a + b, 1};
    x = {-orib.a, -4orid.a + b, -1};
    y = {-orib.a, -2orib.a + b, -1};
    z = {orid.a, 2orid.a + b, -1};
    Chop[{v, w, x, y, z}]
)
translate[{a_, b_, -1}] := (
    v = {oria.a, b, -1};
    w = {-oria.a, -2oric.a + b, -1};
    x = {-oria.a, -4oric.a + b, 1};
    y = {-oria.a, -2oria.a + b, 1};
    z = {oric.a, 2oric.a + b, 1};
    Chop[{v, w, x, y, z}]
)
translate[list_] := (
    Flatten[Map[translate, list], 1]
)
rotexpand[{a_, b_, c_}] := (
    x = {oria.a, rotloc.b, c};
    x
)
rotexpand[list_] := (
    Map[rotexpand, list]
)
substitution[a_] := (
    translate[rotexpand[a]]
)
TileSubstitutionPlot[n_] := (
    pinwheeltiling = Nest[substitution, startpoint, n] /. {a_, b_, c_} →
        {{Line[{b + a - c*ninety.a, b - a - c*ninety.a}],
        Line[{b - a - c*ninety.a , b - a + c*3(ninety.a)}],
        Line[{ b - a + c*3(ninety.a), b + a - c*ninety.a }]}};
    Show[Graphics[pinwheeltiling], AspectRatio → Automatic, PlotRange
        → All, Axes → False]
)
Attributes[TileSubstitutionPlot] = Listable
```

```
PinwheelPoints[n_] := (
    pinwheeltiling = Nest[substitution, startpoint, n] /. {a_, b_, c_} → b
)
PinwheelPoints[5] >> pinpoints5
```

The value 5 appears in the final line of code above merely as an example value of n. The pinpoint5 file generated by the above code is loaded in the code below and its diffraction is calculated and displayed:

```
z5 = <<pinpoints5;
Diff[lambda_, len_, exp_, u_, v_] := (
    g = ((Abs[Sum[Exp[2*Pi*I*{u, v}.lambda[[i]]], {i, len}]])^2)
        /(4*5^(exp))
)
PlotDiff[lambda_, len_, exp_, r_, poi_] := (
    Plot3D[Diff[lambda, len, exp, x, y], {x, -r, r}, {y, -r, r},
        PlotPoints → poi, Mesh → False, PlotRange → All]
)
```

The following line was used to generate Figure 15:

```
Timing[PlotDiff[z5, Length[z5], 5, 1, 401]]
```